INVESTIGATION OF CO OXIDATION KINETICS OVER GOLD CATALYSTS

by

Caner Ülgüel

B. S. in Ch.E., Gazi University, 2008

Submitted to the Institute for Graduate Studies in
Science and Engineering in partial fulfillment of
the requirements for the degree of
Master of Science

Graduate Program in Chemical Engineering

Boğaziçi University

2011

to my family

ACKNOWLEDGEMENTS

Firstly, I would like to express my sincere thanks to my thesis supervisor Prof. Zeynep İlsen Önsan and my thesis co-supervisor Prof. Ramazan Yıldırım for their guidance, interest, continuous encouragement and clear-sighted suggestions. It was a great honor for me to work with them during my graduate thesis.

My sincere gratitude is due to my thesis committee members, Prof. Ayşe Nilgün Akın, Assoc. Prof. Ahmet Kerim Avcı and Assist. Prof. A. Kerem Uğuz who devoted their valuable time to read and commented on my thesis.

Very special thanks to Melek Selcen Başar and Aybüke Leba for their friendship and giving me endless support, valuable advice and motivation from the very beginning of my graduate study and experiments. I was very lucky to work with the CATREL team, Murat Erol, A. İpek Paksoy, M. İrfan Hösükoğlu, Merve Eropak, Nilay Aktürk, Ali Uzun, Vasfiye Çimenoğlu, and with Okan Yüzüak, Gülsüm Ersoy, Bahar Nalbantoğlu, Duygu Kocaman, Şefik K. Ovalı, M. Ünal Güneş, Çağlar Meriçer and Burcu Yoğurtçu. Their support and guidance helped a lot to finish this thesis.

I also wish to express my gratitude to Tuğba Davran Candan as my mentor. Her invaluable experience and will to help has made this study possible.

Cordial thanks for Bilgi Dedeoğlu, Nurettin Bektaş and Yakup Bal for their technical assistance and help.

I wish to thank my family for all their support, patience and encouragement throughout my life. Finally, very special thanks go to Çağrı Yüksel for her emotional support and everlasting inspiration. This thesis would not have been possible without them.

The financial support for this research was provided by TÜBİTAK through project 109M207 and by Boğaziçi University Research Fund through project BAP-09HA508D.

ABSTRACT

INVESTIGATION OF CO OXIDATION KINETICS OVER GOLD CATALYSTS

This experimental study involves preliminary work conducted over 0.5wt%Au/Al_2O_3 and kinetic study of low-temperature CO oxidation over 1wt%Au/1.25-wt%MgO/Al_2O_3 prepared by the homogeneous deposition-precipitation method. Several sets of experiments were carried out to understand the fact that there is no interaction between chemical and physical phenomena. For this purpose, three different total flow rates, 100, 120 and 150 ml/min, were employed in the 90-130^oC temperature range varying the catalyst weight to keep contact time constant in the absence and presence of hydrogen. Kinetic experiments were later conducted at 130^oC and atmospheric pressure using different sets of CO and O_2 concentrations at different catalyst loadings. Molar reactant concentrations in the feed were varied between 2-8 per cent CO and 1-6 per cent O_2 in the absence of hydrogen. Experimental rate data were used to estimate the kinetic parameters of power law and proposed LHHW models using the method of initial rates. The investigation of power law kinetics gave reaction orders of 0.61 and 0.31 with respect to carbon monoxide and oxygen, respectively, and a reaction rate constant of 3.55 $mol.g^{-1}.h^{-1}.atm^{-1}$ at 130^oC. Both power law and LHHW models fit well to the experimental data. Finally, the effects of H_2, CO_2 and/or H_2O addition to the feed on CO conversion in the low temperature oxidation of CO were also investigated. The addition of H_2 or H_2+H_2O to the feed enhance CO conversion whereas the presence of CO_2 has a negative effect.

ÖZET

ALTIN KATALİZÖRLER ÜZERİNDE CO OKSİDASYONU KİNETİĞİNİN İNCELENMESİ

Bu deneysel çalışmada, 0.5%Au/Al_2O_3 katalizörü üzerinde yapılan ön deneyleri ve homojen tortu çöktürmesi yöntemi ile hazırlanan 1%Au-1.25%MgO/Al_2O_3 katalizörü üzerinde gerçekleştirilen düşük sıcaklık CO oksidasyonuna ilişkin kinetik çalışmaları içermektedir. Kimyasal ve fiziksel olaylar arasında herhangi bir etkileşim olmadığını belirlemek için yapılan deneylerde, hidrojen varlığında ve yokluğunda akış hızlarına orantılı katalizör miktarı kullanılarak 90-130^oC sıcaklık aralığında üç farklı akış hızı, 100, 120 ve 150 ml/dak, kullanlıdı. Daha sonra, reaksiyon kinetiğine ilişkin deneyler 130^oC'de ve atmosferik basınçta yapılarak değişik katalizör miktarlarında farklı CO ve O_2 girdi derişimleri kullanıldı. Hidrojen yokluğunda beslemedeki molar reaktant derişimleri CO için yüzde 2-8 arasında, O_2 için yüzde 1-6 arasında değiştirildi. Üssel hız denkleminde ve önerilen LHHW tipi hız modellerinde yer alan kinetik parametreler deneysel hız verileri kullanılarak başlangıç hızları yöntemi ile hesaplandı. Karbon monoksit ve oksijenin reaksiyon mertebeleri sırasıyla 0.61 ve 0.31, ve reaksiyon hız sabiti 3.55 $mol.g^{-1}.h^{-1}.atm^{-1}$ (130^oC) olarak belirlendi. Gerek üssel gerekse LHHW tipi modellerin deneysel verilere çok uygun sonuçlar verdiği görüldü. Son olarak, reaktör girdisine H_2, CO_2 ve/veya H_2O eklenmesinin düşük sıcaklık CO oksidasyonunda CO dönüşmesi üzerindeki etkileri de incelendi. Reaktör girdisine H_2 veya H_2+H_2O eklenmesinin CO dönüşmesini artırdığı, CO_2 eklenmesinin ise olumsuz etkilediği gözlemlendi.

TABLE OF CONTENTS

LIST OF FIGURES

LIST OF TABLES

LIST OF SYMBOLS

d_p	Catalyst particle size
F	Total flow rate
k	Reaction rate constant
K	Numerical value for the equilibrium constant for the reaction
L	Catalyst bed lenght
MW	Molecular weight
P	Partial pressure
R	Universal gas constant
r_{CO}	Reaction rate for CO
T	Temperature
V	Molar Volume
W	Weight of catalyst
W/F	Residence time
X	Conversion
α	Order with respect to CO
β	Order with respect to O_2
ρ	Density

LIST OF ABBREVIATIONS

ATR	Autothermal Reforming
CP	Co-precipitation
CVD	Chemical Vapor Deposition
DP	Deposition Precipitation
HDP	Homogeneous Deposition Precipitation
KOH	Potassium Hydroxide
MEA	Membrane Electrode Assembly
MCFC	Molten Carbonate Fuel Cell
MS	Mass Spectrometer
PAFC	Phosphoric Acid Fuel Cell
PD	Photo Deposition
PEMFC	Proton Exchange Membrane Fuel Cell
POX	Partial Oxidation
PROX	Preferential Oxidation
ppm	Parts per million
SOFC	Solid Oxide Fuel Cell
SR	Steam Reforming
YSZ	Yttria Stabilized Zirconia

1. INTRODUCTION

Hydrogen, which is a clean, highly efficient and environmentally friendly fuel, has attracted much attention in recent years especially as the fuel for proton exchange membrane (PEM) fuel cell technology (Naknam *et al.*, 2009). Hydrogen is mostly produced by using fossil fuels, such as natural gas and coal. However, these fuels have a limited reserve, and in addition, they release greenhouse gases during the hydrogen production process (Bartels *et al.*, 2010). Therefore, new energy technologies making use of renewable energy resources are gaining much popularity to overcome the non-sustainable nature of current energy systems. Among the alternatives available, hydrogen has an outstanding clean energy nature, which does not produce CO_x and NO_x when used as a fuel, because of its reducing effect in the emissions of these pollutants (Vizcaino *et al.*, 2007).

Fuel cells are electrochemical devices that directly convert chemical energy stored in fuels such as hydrogen to electrical energy (Wang *et al.*, 2011). The fuel cell technology provides significant improvements to generate clean and efficient power and is an important alternative to conventional techniques. Fuel cells with special characteristic can be used in different kind of industries, especially in mobile applications, since the latest internal combustion engine technology coupled with converters cannot completely eliminate emissions. Fuel cell powered electrically driven vehicles, on the other hand, can produce nearly zero emission (Avcı *et al.*, 2002).

Among the types of fuel cells receving major efforts of research, the proton exchange membrane fuel cell (PEMFC) has the widest utilization area in industrial applications. PEMFC is set up using polymer electrolyte membranes as proton conductor and Platinum (Pt)-based materials as catalyst. Noteworthy properties of PEMFCs cover low operating temperature, high power density, and easy scale-up, enabling them to be utilized as clean and renewable power sources for transportation, stationary, and portable applications (Wang *et al.*, 2011).

The production of hydrogen is of great interest from hydrocarbons and alcohols via several production methods including steam reforming, partial oxidation, and auto-thermal reforming (Seo *et al.*, 2009). In these processes, the exit gas stream includes significant amounts of CO and it is treated in water-gas-shift (WGS) reactors to obtain hydrogen rich gas mixtures. However, the hydrogen stream from the processor contains 1 vol.% CO, which must be lowered below 10 ppm since the anode catalyst (generally Pt) of the fuel cell is very sensitive to CO poisoning particularly at low operating temperatures (Kotobuki *et al.*, 2005).

Among other approaches used for the removal of CO, such as membrane separation and methanation, preferential oxidation of CO in H_2 rich streams (PROX) has advantageous features such as simple design, cost effective application and low hydrogen consumption (Yu *et al.*, 2007). Compared to PROX, Pd-based membrane separation requires high pressure difference and quite a high temperature for hydrogen diffusion, and methanation consumes three moles of hydrogen to convert per mole of carbon monoxide resulting in a reduction in the amount of hydrogen (Holladay *et al.*, 2004).

The oxidation of the carbon monoxide present in the reformate stream produces carbon dioxide over a suitable catalyst using molecular oxygen in PROX which is an exothermic process. In the last years, researchers have conducted numerous studies for finding and developing catalysts that are suitable for the PROX reaction. It is important that such a catalyst should be active for the oxidation of CO and inactive for the undesired oxidation of H_2, in the 80-250^{o}C temperature range. Noble metal catalysts, including Au, Pt, Ru, Rh or Ir have been widely examined for this purpose (Moreno *et al.*, 2008). Especially Au catalysts supported on metal oxides such as Al_2O_3, MnO_x, Fe_2O_3, MgO-Al_2O_3 were found to be very active for CO oxidation reaction since they also promoted the activity of the Au catalyst (Luengnaruemitchai *et al.*, 2004).

Gold was considered to be a catalytically inactive material for a long time because of its deep-lying valence d band and very diffuse valence s and p orbitals (Chang *et al.*, 2007). The attention for supported Au catalysts has increased substantially since Haruta *et al.* found that these kinds of catalysts are active for low-temperature CO oxidation. Many supported gold-based catalysts such as Au/TiO_2, Au/ ZrO_2, Au/Fe_2O_3, Au/CO_3O_4, Au/NiO

and Au/Al_2O_3 have been prepared by various methods and tested for preferential CO oxidation (Zou *et al.*, 2007; Lian *et al.*, 2005).

The mechanism of CO oxidation in hydrogen-rich streams is described by the Langmuir–Hinshelwood (L–H) model. It is suggested that CO and oxygen molecules are closely co-adsorbed on gold, and that CO oxidation occurs over gold clusters through L–H mechanism rather than Eley–Rideal (E–R) mechanism. CO can adsorb either on cationic gold or metallic gold and those having low-coordination number can react with O_2 co-adsorbed on the same gold sites (Chang *et al.*, 2008). Although some work has already been done to understand the mechanism and kinetics of CO oxidation over Au catalysts to suggest corresponding possible mechanisms, a definitive conclusion has not yet been reached.

The aim of the present study is to investigate kinetics of both CO oxidation and selective CO oxidation over $Au/MgO/Al_2O_3$ catalysts prepared by homogenous deposition precipitation. The reaction tests were carried out in a microflow reaction system equipped with automated gas flow system, and a temperature controlled reactor. Firstly, for the preliminary experiments, different total flow rates were used to determine the mass transfer effect in the temperature range of 90-130^oC. Then, the effects of the reaction parameters such as stoichiometric and non-stoichiometric CO/O_2 ratios, H_2 concentration, CO_2 and H_2O concentrations on the CO conversion and the reaction rate were evaluated at 130^oC, and a kinetic study was conducted.

The present work is comprised of five chapters. Section 2 involves a literature survey including a brief introduction to fuel cells, hydrogen production methods, preferential CO oxidation and the catalysts employed in PROX. Section 3 involves all experimental systems, catalyst preparation procedures, and the conditions for kinetic measurements. The results obtained in the experiments are presented and analyzed in Section 4. Finally, the conclusions of this study and recommendations for future work are discussed in Section 5.

2. LITERATURE SURVEY

2.1. Fuel Cell Technology

Increasing environmental problems, limited fossil fuel resources and the geopolitical dependence on crude oil are enormous challenges for our societies. According to energy experts from all over the world, fuel cell and hydrogen energy technologies will play an important role in the future energy economy (Neef, 2009).

Fuel cells are electrochemical devices in which the chemical energy stored in fuel is converted directly to electrical energy through an electro-catalytic process. Among the various renewable energy sources, fuel cell has attracted the attention due to its outstanding features such as higher efficiency, cleanliness and cost-effective supply of power; fuel cells do not need to recharge, and unlike batteries, can produce electricity continuously as long as they are supplied with fuel (Thiam *et al*., 2011; Varigonda and Kamat, 2006).

A fuel cell comprises an electrolyte layer in contact with two electrodes on either side. The hydrogen, as a fuel, is fed continuously to anode electrode while the oxygen from air is fed continuously to the cathode electrode. At the anode terminal the hydrogen fuel is separated into positive ions and negative ions. The intermediate electrolyte membrane allows only the positive ions to flow from anode to cathode side acting as an insulator for electrons. These electrons want to recombine on the other side of the membrane for the system to become stable, for which the free electrons pass to the cathode side through an external electrical circuit. The recombination of the positive and negative ions with oxidant occurs at the cathode to produce depleted oxidant (or) pure water (Kirubakaran *et al*., 2009).

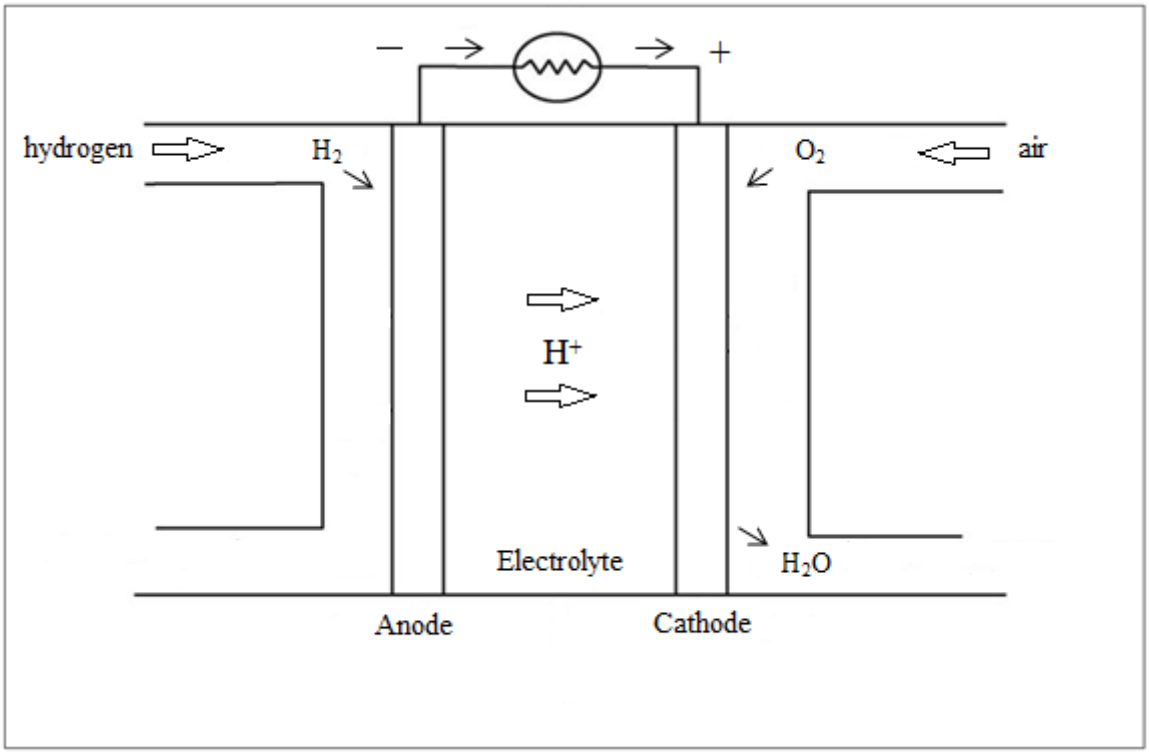

Figure 2.1. Schematic of a fuel cell.

2.1.1. Types of Fuel Cells

Fuel cell technologies can be classified in many ways, for example, by the operating temperature, fuel type, oxidizer type, or charge carrier. Each type of fuel cell has its own advantages and disadvantages compared to the others. Mostly there are five types of fuel cell including solid oxide fuel cell (SOFC), molten carbonate fuel cell (MCFC), phosphoric acid fuel cell (PAFC), alkaline fuel cell (AFC), and proton exchange membrane fuel cell (PEMFC) (Thiam *et al*., 2011; Schoots *et al*., 2010).

The solid oxide fuel cell (SOFC) and the molten carbonate fuel cell (MCFC) are high temperature fuel cells operating at around 600-1000^{o}C. SOFC uses dense yttria stabilized zirconia (YSZ), which is a solid ceramic material, as its electrolyte. Since MCFC has high operating temperatures, it does not need metal catalyst. Moreover, both of them do not require a separate reformer. However, there are also several critical problems, such as slow start up, high cost and intolerance to sulfur content of the fuel cell (Kirubakaran *et al*.,

2009). The phosphoric acid fuel cell (PAFC) and the alkaline fuel cell (AFC), on the other hand, operate at low temperatures around 100-175^{o}C. The former uses liquid phosphoric acid as an electrode. The latter employs an aqueous solution of potassium hydroxide (KOH) as an electrolyte (Sollogoub *et al*., 2009).

Among the fuel cell types, proton exchange membrane fuel cell (PEMFC) is considered as one of the most promising technology that can produce efficient and environmentally friendly energy for powering electrical vehicles (Kaytakoğlu *et al*., 2007). The PEMFC operates at low temperatures around 100^{o}C. Its lower operating efficiency (40-45%) and use of high cost platinum catalysts are seen as the major drawbacks. It is also intolerant to carbon monoxide (Kirubakaran *et al*., 2009). Its noteworthy features including low operating temperature, high power density, and easy scale-up make PEMFC a promising candidate as the next generation power source for vehicular, stationary, and portable applications (Wang *et al*., 2011).

The membrane (PEM) consists of a perfluorinated polymer backbone with sulfonic acid side chains. This material becomes an excellent protonic conductor when it is fully humidified. The membrane, two layers of catalyst (platinum supported on carbon particles) and two gas diffusion electrodes (teflonated porous carbon cloth or paper) are assembled into a membrane electrode assembly (MEA). The MEA is positioned between two current collectors which also run as gas distributors for the fuel (hydrogen) and oxidant (oxygen or air). The hydrogen rich fuel flows into the fuel cell on the anode side. It diffuses through the porous anode gas diffusion layer and comes in contact with the anode catalyst layer. Here it decomposes into protons and electrons according to:

$$2H_2 \rightarrow 4H^+ + 4e^- \qquad (2.1)$$

The protons go through the PEM at the center; the electrons flow through the anode gas diffusion layer to anode current collector and into the electric load attached. Electrons move towards the cathode catalyst layer through the cathode current collector and gas diffusion layer. The oxygen in the cathode gas stream diffuses through the cathode gas diffusion layer towards the cathode catalyst layer where it comes together with the protons and electrons to from water (Yu *et al*., 2009):

$$O_2 + 4H^+ + 4e^- \rightarrow 2H_2O \quad (2.2)$$

In a fuel processor, there are three catalytic reactions existing in series in order to produce pure hydrogen to be fed to a PEM fuel cell: (i) reforming of hydrocarbons to hydrogen; (ii) water-gas shift (WGS) reaction for decreasing carbon monoxide concentration while increasing hydrogen concentration; (iii) preferential carbon monoxide oxidation, which reduces carbon monoxide in the reformer product to ppm levels (Çağlayan *et al*., 2005).

2.2. On-board Hydrogen Production Methods

Hydrogen is regarded as the most viable energy carrier in the future because of its clean, renewable, and non-polluting nature. Hydrogen has become more popular due to the technological advances in hydrogen utilization like fuel cells and is characterized as a next generation fuel. Hydrocarbon sources for hydrogen production via catalytic reforming processes are natural gas, gasoline, alcohols, and biomass (Youn *et al*., 2009).

Hydrogen can be produced from hydrocarbons for PEMFC applications by several methods comprising steam reforming (SR), direct partial oxidation (POX), and autothermal reforming (ATR) (Önsan, 2007):

SR: $C_nH_mO_p$ + steam → carbon oxides + hydrogen $\Delta HR > 0$ (2.3)

POX: $C_nH_mO_p$ + air → carbon oxides + hydrogen + nitrogen $\Delta HR < 0$ (2.4)

ATR: $C_nH_mO_p$ + steam + air → carbon oxides + hydrogen + nitrogen $\Delta HR \leq 0$ (2.5)

Steam reforming is an endothermic reaction and thus requires energy input, which makes transient operation difficult. It also has a lower operating temperature than POX and ATR, and produces the reformate with a high H_2/CO ratio (~3:1) which is favourable for hydrogen production. In contrast to steam reforming, partial oxidation and autothermal reforming processes do not entail indirect heating. Moreover, they provide faster start-up time and better transient response. Compared to partial oxidation and autothermal

reforming, catalytic steam reforming offers higher hydrogen concentrations (Perez-Hernandez *et al*., 2007; Ersöz *et al*., 2006). A reformate stream produced using pure SR includes 70%-80% H_2 on a dry basis, whereas pure POX produces a reformate stream containig 35%-45% H_2. Except for methanol SR, in all processes for hydrogen production using hydrocarbons, sizeable water-gas shift converters are needed for reducing the CO concentration and increasing the H_2 content of the reformate (Önsan, 2007).

2.3. Preferential CO Oxidation (PROX)

The exit gas stream coming out of the WGS converter contains 40-75% H_2, 15-20% CO_2, 0.5-2% CO, and 10% H_2O. Since the CO in the gas stream poisons the Pt-based anode catalyst of the PEMFC, its content must be reduced to less than 10 ppm (Şimşek *et al*., 2007).

There are several effective ways to reduce the CO content to ppm levels. (i) Diffusion of hydrogen through a Pd/Ag membrane, but this requires high pressure differentials and fairly high temperatures and is also costly. (ii) CO methanation, which consumes 3 molecules of hydrogen to convert one mol of CO leading to a decrease in the amount of the desired product and, also, about 20 vol% CO_2 is formed. Accordingly, (iii) selective oxidation of carbon monoxide, also known as preferential oxidation of carbon monoxide (PROX), which takes place in the presence of CO_2 and H_2O with minimum H_2 oxidation, is considered as the most promising and economical method (Trimm and Önsan, 2001; Zhou *et al.*, 2006).

The crucial requirements for the PROX reaction are high CO oxidation rate and high selectivity. Selectivity is important for the competing H_2 oxidation because it may result in a decrease in the overall fuel cell efficiency. Besides oxidation of both CO and H_2, methanation and WGS reactions can also happen simultaneously. Methanation is the detrimental reaction since it consumes H_2 and should be avoided whereas WGS reaction produces H_2 while decreasing CO (Souza *et al.*, 2007).

PROX: $CO + 0.5O_2 \rightarrow CO_2$ ΔH= −283.0 kJ/mol (2.6)

$H_2 + 0.5O_2 \rightarrow H_2O$ ΔH= −242.0 kJ/mol (2.7)

Methanation: $CO + 3H_2 \rightarrow CH_4 + H_2O$ ΔH= −283.6 kJ/mol (2.8)

WGS: $CO + H_2O \rightarrow CO_2 + H_2$ ΔH= −41.4 kJ/mol (2.9)

It is significant that CO content should be decreased from 0.5-1 mol% to 10-50 ppm before the H_2 stream enters the PEM fuel cell and this can be achieved placing a preferential CO oxidation (PROX) reactor right after the low temperature water-gas-shift converter to produce CO-free hydrogen (Soyal-Baltacıoğlu *et al.*, 2007).

Oxygen and carbon monoxide compete for the same sites at low temperatures and low O_2/CO ratios and oxygen adsorption needs more sites. Under these conditions, carbon monoxide adsorption dominantly occurs on the metal surface, thus, preventing O_2 adsorption and surface reaction. On the other hand, oxygen is held too strongly to be displaced by carbon monoxide over base-metal oxide catalysts at low temperatures. Therefore, the effective low-temperature CO oxidation catalyst should provide suitable sites for both CO chemisorption and the simultaneous dissociative adsorption of oxygen at low temperatures (Trimm and Önsan, 2001).

There are three obvious possibilities that can be considered for an efficient PROX system, one of which is to find a catalyst that adsorbs CO but not H_2, so favoring selective CO oxidation. It is also possible to select a temperature at which CO is oxidized but H_2 is not. As the last possibility, a catalyst may be found where both CO and H_2 are oxidized, but the kinetic parameters lead to preferential oxidation of CO at the cost of only small amounts of H_2 loss. In all cases, it is of great importance to control oxygen-carbon monoxide ratio and temperature of the reaction (Trimm and Önsan, 2001).

A selective CO oxidation catalyst in streams with excess H_2 must meet the requirements summarized as follows:

- high CO oxidation activity at low temperatures,
- high oxidation selectivity for CO against H_2,
- wide temperature window for CO conversions greater than 99% (TW99), and
- good tolerance for the presence of CO_2 and H_2O in the feed.

The selectivity of a catalyst for CO oxidation against H_2, which is high at low temperatures, decreases with rising temperature since H_2 oxidation competes at high temperatures. Accordingly, low-temperature activity of a catalyst is very important for the highly selective oxidation of CO (Park, 2004).

The catalysts used for the PROX system can be grouped into non-noble metal oxides, Au-based catalysts, Pt-based catalysts and Ru-based catalysts (Kim and Park, 2010). The noble metals (platinum, palladium, ruthenium and gold etc.) have an advantage of good activity for CO oxidation. However, these metals have drawbacks such as high cost, limited availability, decreasing selectivity at high temperatures and requirement of two-stage PROX reactors to reduce CO (Park *et al.*, 2005).

Platinum supported catalysts are used in a fuel processors because of their ability to operate at high temperatures, their stability for long term operation and their high resistance to deactivation by CO_2 or H_2O (Lucas-Consuegra *et al*., 2010). The effects of magnesium on platinum catalysts used in preferential CO oxidation for PEMFC applications were studied. From experimental results, it was seen that Pt–Mg/Al_2O_3 catalysts are superior to Pt/Al_2O_3 catalysts in H_2-rich streams. Reaction activity increases since Mg addition improves the concentration of hydroxyl groups on the surface of Pt catalysts. In the presence of water in the feed stream, the selectivity of Pt-Mg/Al_2O_3 for preferential CO oxidation is decreased. The reason for this can be attributed to water preventing CO from being adsorbed onto the surface of the Pt metal (Cho *et al.*, 2006).

Ko *et al.* (2006) examined supported Pt catalysts (Pt/γ-Al_2O_3, Pt-Ni/γ-Al_2O_3, and Pt-Co/γ-Al_2O_3). Their results showed that Pt–Ni/γ-Al_2O_3 had the highest CO conversion among other catalysts with a high CO_2 selectivity over a wide reaction temperature range.

This catalyst also showed the best performance in the presence of 2 vol.% H_2O and 20 vol.% CO_2.

Since the noble-metal catalysts have some drawbacks, attention has been drawn to the base-transition metal catalysts. Cerium oxide is well known to have a high oxygen exchange capacity, which is related to the capacity of cerium to change oxidation states reversibly between Ce^{4+} and Ce^{3+} by receiving or giving up oxygen (Chen *et al*., 2006). The catalytic activity and CO oxidation selectivity of $CuO–CeO_2/\gamma\text{-}Al_2O_3$ in selective CO oxidation in the presence of excess H_2 were investigated. Effects of Co addition as a promoter on the catalytic activity and CO oxidation selectivity were determined. $CuO\text{-}CeO_2/\gamma\text{-}Al_2O_3$ incorporating Co of 0.2 wt.% was found to be the most active catalyst with CO conversion >99% in the wide temperature window of 150–220^oC (Park, 2004).

Much research has been carried out related to the combinatorial catalysis especially of Pt and Pd for CO oxidation. Using bimetallic systems has a strong enhancement effect on the properties of the catalyst, which is quite an attractive method. Parinyaswan *et al.* (2006) investigated Pt-Pd supported on ceria catalysts prepared by impregnation in different Pt-Pd ratios, (1:1), (1:7), (1:9), for preferential oxidation of CO in the presence of hydrogen in the temperature range of 50-190^oC and atmospheric pressure. It was found that 1% (1:7) $Pt\text{-}Pd/CeO_2$ (sol–gel) exhibited higher activity than the other catalysts examined.

The use of zeolites (MOR, ZSM-5, FAU and ETS-10) as a support for Pt catalysts in selective CO oxidation has also been studied, and it was found that the best results were obtained with Pt-FAU catalysts, showing stable catalytic activity and complete conversion of CO at 439K (Sebastian *et al.*, 2009).

Palladium catalysts supported on various support materials, ZnO, Ga_2O_3, SiO_2, CeO_2, In_2O_3, and Al_2O_3, were studied for selective CO oxidation with O_2 in H_2-rich gas. Among the catalyst examined, the most active catalyst was determined to be Pd/ZnO. The Pd species existed in the form of a PdZn alloy on this catalyst and the alloy was more effective for the reaction compared with metallic Pd species of the other catalysts tested (Iwasa *et al.*, 2008).

Rubidium supported aluminum oxides with different crystalline phases, viz. α-Al_2O_3, κ-Al_2O_3, γ-Al_2O_3, η-Al_2O_3, δ-Al_2O_3 and θ-Al_2O_3, prepared by the incipient wetness method, were investigated by Kim and Park (2010) for selective CO oxidation in a hydrogen-rich stream. For comparison, complete CO oxidation in the absence of H_2 was also carried out over the same catalysts. Ru/α-Al_2O_3 showed the highest CO conversion among the tested catalysts, especially at low temperatures. The experimental results showed that Ru/α-Al_2O_3 reduced the CO content to less than 10 ppm even in the presence of H_2O and CO_2 over a wide temperature range.

Iridium has attracted little interest as a catalyst in the CO oxidation reaction, but recent researches have highlighted high activity for iridium supported on Al_2O_3, SnO_2, TiO_2, and CeO_2 in selective CO oxidation (Tomska-Foralewska *et al*., 2011). Huang *et al.* (2007) performed a study on iridium catalysts deposited on different oxide supports (CeO_2, TiO_2, Al_2O_3 and MgO) for the preferential CO oxidation under excess H_2 conditions. The Ir/CeO_2 catalyst exhibited excellent performance in PROX. They also found that the Ir/CeO_2 catalyst prepared by both homogeneous deposition-precipitation (HDP) and deposition-precipitation (DP) methods showed high activity.

In order to investigate the effects of temperature and the presence of CO_2 and H_2O in the feed, Pt-SnO_2/Al_2O_3 sol–gel catalysts were employed for selective CO oxidation in hydrogen rich streams. Complete conversion was achieved over the 1wt%Pt-3 wt% SnO_2/Al_2O_3 catalyst at 110^{o}C. CO conversion decreased significantly in the presence of CO_2 while H_2O in the feed increased CO conversion. Changing the temperature from 110 to 120 and 130^{o}C resulted in slight activity loss, although the conversion was still higher than 95% (Uysal *et al.*, 2006).

Pt-Co-Ce/Al_2O_3 catalyst prepared by incipient to wetness co-impregnation technique was used for the selective low-temperature oxidation of CO in excess hydrogen. 100% CO conversion was obtained over 1.4wt%Pt-1.25wt%Co-1.25wt%Ce/Al_2O_3, with significantly higher selectivity at 90^{o}C (İnce *et al*., 2005).

Soyal-Baltacıoğlu *et al.* (2007) performed a kinetic study of low temperature CO oxidation over sequentially impregnated 1wt%Pt-0.25wt%SnO_x supported on HNO_3-

oxidized activated carbon (AC3). Intrinsic kinetic data were obtained in the initial rates region at 383 K in the absence and presence of 5-45 mol% H_2 in the feed. A power-function rate expression with positive dependence on CO (0.96) and negative dependence on oxygen (-0.31) was obtained indicating that the reaction takes place on a surface that is predominantly covered by adsorbed oxygen with relatively weak CO adsorption.

2.4. CO Oxidation over Gold based Catalyst

Gold has, until recently, been considered as one of the least catalytically useful metals because it has chemical inertness and the difficulty to achieve a high dispersion on common support materials (Centeno *et al*., 2002). In 1989, attention has been drawn to gold catalysts when Haruta *et al*. documented the outstanding features of supported gold to effectively catalyze oxidation reactions at low temperatures (Calla *et al*., 2006).

Haruta and coworkers elucidated the mechanism of CO oxidation on gold. There are three main models favoring; (1) the metal–support interaction (interface effect), (2) the presence of low-coordinated atoms on the nanoparticles (geometry effect), or (3) the low dimensionality of the gold structures (quantum size effect) (Azar *et al*., 2006).

The activity of the supported gold catalyst in CO oxidation at low temperature depends on various factors including the size of Au particles, the nature of supports, the preparation methods, the preparation parameters and the pretreatment conditions (Chang *et al*., 2007). There is strong correlation between catalytic activity and gold particle size. Smaller particle sizes of 2-3nm enhance the catalytic performance of gold catalyst (Trimm and Önsan, 2001).

It has been reported that different CO oxidation kinetics can be observed when gold nanoparticles are supported on different metal oxides (Calla *et al*., 2006). Al_2O_3 is one of the most common oxides used as a support in industrial catalytic processes for selective oxidation of CO (Zou *et al*., 2007).

In addition, support materials can be catagorized into two types as active (TiO_2, Fe_2O_3, CeO_2, MnO) or inactive (SiO_2, MgO, Al_2O_3). Active supports increase catalytic

activity by providing oxygen atoms; moreover, they also have the ability to improve the stability of small gold particles. The reactivity of gold clusters on inactive supports is related to high metal dispersion and the presence of a low-coordinated gold surface sites (Chang *et al*., 2007).

Rossignol *et al.* (2005) prepared gold catalysts supported on different metal oxides, Al_2O_3, ZrO_2, and TiO_2. They were employed in preferential CO oxidation in excess hydrogen in the temperature range of 25-420^oC. An increment in CO conversion was observed at low temperatures, the extent of this boost was dependent on support identity. Hence, the reactivity for CO oxidation was found in the order of Au/Al_2O_3 <Au/ZrO_2 <Au/TiO_2.

In addition to particle size, the choice of the preparation method is of great significance for the performance of gold catalysts. These methods can be classified as co-precipitation, deposition–precipitation (DP), chemical vapour deposition (CVD), laser vaporization, modified impregnation, and photo-deposition (PD) method. DP method is the simplest and most cost-effective method to prepare gold catalysts (Yang *et al*., 2009). Wang *et al*. (2003) reported that co-precipitation (CP) and deposition precipitation (DP) are the most commonly employed methods. CP is easy to control with a powder sample obtained. However, DP has advantage over CP in that all of the active components remain on the surface of the support and none of the active gold component is buried within. However, it is not easy to control the properties of a supported gold catalyst prepared by DP, because they are highly sensitive to preparation condition.

MgO enables the preparation of small and stable Au particles on γ-Al_2O_3 with high surface area; thus improves the low temperature CO oxidation. Addition of MnO_x and FeO_x to $Au/MgO/Al_2O_3$ enhances CO conversion, especially at low temperatures. In addition, the CO_2 selectivity is found to benefit considerably from the presence of both oxides. The increase in CO oxidation activity is ascribed to the implementation of new routes for supplying active oxygen, e.g., via lattice oxygen. At low temperatures, suppression of H_2 oxidation also results in the better CO_2 selectivity (Grisel *et al*., 2002).

Gold-based catalysts are resistant to deactivation by water or carbon dioxide (Trimm, 2005). Schubert *et al*. (2004) investigated the effects of CO_2 and H_2O on the preferential CO oxidation in hydrogen rich gases using Au/α-Fe_2O_3 catalyst at 80^oC. From the experimental results, it was concluded that CO_2 has negative effect on the reaction, and reduces both CO oxidation rate and CO oxidation selectivity. Addition of H_2O results in opposite effects. It increases the selectivity by suppressing the H_2 oxidation reaction; hence it improves the CO oxidation rate. Catalyst deactivition is significantly reduced and this is attributed to the transformation of surface carbonates into thermally less stable bicarbonate species.

Ceria-supported Au catalysts for selective CO oxidation for polymer electrolyte membrane fuel cell (PEMFC) application were investigated by Panzera *et al*. (2004). A nearly complete CO conversion was achieved at 120^oC, whereas CO_2 selectivities obtained was low, around 40% in the entire temperature range of 80-120^oC. Both CO conversion and CO_2 selectivity were negatively affected by CO_2 in the feed stream. Moreover, it was stated that the addition of ceria to γ-Al_2O_3 changes in the acid-base properties of the support surface, providing well-established catalytic properties of the Ce^{3+}/Ce^{4+} pair, which makes CeO_2/Al_2O_3 solids a very promising material to prepare gold catalysts with high catalytic activity and high metal dispersion (Centeno *et al*., 2002).

Laguna *et al.* (2010) examined iron effect on ceria supports containing different molar percentages of Fe (0%, 10%, 25%, and 50%). CeFe10 was chosen as support for preparing the gold catalyst, because the Ce-Fe interaction in the lowest iron content (10%) occurs through the formation of a solid solution, which is determined to be very active for PROX reactions, especially at low temperatures compared with Au/CeO_2. H_2O and CO_2 in the feed do not change the catalytic performance of the Au/CeFe10 catalyst.

The character of Au species on an Au/$FePO_4$ catalyst was examined after oxidative and reductive pretreatments. Oxidative pretreatment (in O_2) results in cationic Au species reduced by CO. In situ reduction of the cationic Au during CO oxidation generates metallic Au that is active for CO oxidation. Reductive pretreatment (in H_2) produces metallic Au species that are more active for CO oxidation than those on an oxidatively pretreated catalyst (Li *et al*., 2009).

In the report by Qian *et al*. (2010), the effect of NaOH additive on the catalytic activity of Au/SiO_2 catalyst was investigated. It was observed that catalyst activity is substantially enhanced in catalyzing CO oxidation at temperatures below 150^oC. Both the particle size distribution and the electronic structure of Au nanoparticles were found to be similar in Au/SiO_2 and $Au/NaOH/SiO_2$ catalysts, proving that hydroxyls on ‘‘inert’’ Au nanoparticles can induce the activation of O_2 for CO oxidation.

Second metal addition changes drastically the catalytic properties of a catalyst, even when the second metal is inactive for the reaction. In order to provide improvement for the catalyst, bimetallic or multicomponent and small amounts of additives are put in as promoters or inhibitors. In the light of the information stated above, the alloy formed between a group-VIII metal such as platinum and a group-IB metal such as gold changes the catalytic behavior as compared to the monometallic phase. Pt-Au catalysts supported on Al_2O_3 or TiO_2 and SiO_2 were prepared. The results of the experiments showed that these catalysts have high activity, selectivity, and high activity per active site (Vazquez-Zavala *et al*., 2000).

Hao *et al*. (2009) studied the performance of supported gold catalysts, analyzing catalyst deactivation. Deactivation of supported gold catalysts was attributed to the reduction and aggregation of the gold, to other morphological changes in gold clusters, and to the reduction of the support surface. The most commonly suggested causes of deactivation were given as sintering of gold clusters and accumulation of carbonate-like species such as carbonates, bicarbonates, carboxylates, and formates.

The effect of moisture on CO oxidation over Au/TiO_2 has been studied over a wide range of concentrations. The amount of moisture adsorbed on the catalyst rather than the moisture content in the gas phase affects the activity, suggesting that low-temperature CO oxidation over gold catalysts involves water-derived species on the catalyst surface (Date and Haruta *et al*., 2001).

The cooling effect was examined by Szabo *et al*. (2007) in selective CO oxidation, changing the atmosphere of cooling from an inert gas to H_2 after reduction in hydrogen at 350^oC. Au/MgO is found to have higher activity after cooling in helium, whereas

Au/Al_2O_3 exhibited the opposite effect, higher activities were measured after cooling in hydrogen.

Kinetics of selective CO oxidation in hydrogen-rich streams was investigated over Au/Al_2O_3 prepared by homogeneous deposition-precipitation. The effects of concentrations of CO and O_2 on CO conversion and reaction rate were considered at temperatures of 90-130°C. It was found that decreasing the Au content from 1 to 0.5 per cent showed negative effects on catalytic activity. Decreasing the temperature from 130 to 110^{o}C increased the activity of the catalyst, resulting in a decrease in the CO conversion at 90^{o}C (Demir, 2009).

Tezcanli (2008) investigated the effects of various promoters (Ce, Co, Ni, Mg, Mn and Fe) on the activity Au/Al_2O_3 catalysts for preferential CO oxidation. The metal oxide promoter was loaded onto the alumina support by using the incipient-to-wetness impregnation method while the homogeneous deposition-precipitation method was employed for the deposition of gold nanoparticles. CO conversions obtained on 1.25wt%Mg promoted samples were close to samples having 2.5 wt% Mg. However, a decrease in activity was observed when the Mg wt% was increased to 5 at all temperatures. Maximum CO conversion was achieved at 50^{o}C with 1wt%Au-1.25wt %MgO/Al_2O_3.

2.5. Kinetics of CO Oxidation over Supported Gold Catalysts

The elementary steps of the proposed reaction mechanisms of CO oxidation over Au based catalysts given in the literature together with the stoichiometric coefficients of each elementary step in the mechanisms considered are presented in Table 2.1. In the table, (∗) denotes pure Au sites, whereas (•) denotes the Au-support interface.

2.5.1. Reaction Path A

Reaction path A is an Eley-Rideal-type (E-R-type) mechanism, and CO adsorbed on Au (CO∗) reacts with O_2 in the gas phase to form reaction intermediate (COOO∗) (Steps 1 and 4 in Table 2.1). This reaction intermediate then decomposes into CO_2 and O∗ (Step 5

in Table 2.1). The remaining O atom adsorbed on Au reacts with another CO molecule for the production of the second CO_2 molecule (Step 3 in Table 2.1).

Table 2.1. Elementary steps and their stoichiometric coefficients involved in the reaction paths considered (Davran-Candan, 2011).

Elementary Step	**A**	**B**	**C**	**D**	**E**	**Step**
	σ_A^*	σ_B^*	σ_C^*	σ_D^*	σ_E^*	**Number**
$CO_{(g)} + * \underset{k_{-1}}{\overset{k_1}{\leftrightarrow}} CO*$	2	2	2	2	2	1
$CO* + O_{2\,(g)} \overset{k_2}{\rightarrow} CO_{2\,(g)} + O*$	0	0	0	0	0	2
$CO* + O* \overset{k_3}{\rightarrow} CO_{2\,(g)} + 2*$	1	1	1	1	2	3
$CO* + O_{2\,(g)} \overset{k_4}{\rightarrow} COOO*$	1	0	0	0	0	4
$COOO* \overset{k_5}{\rightarrow} CO_{2\,(g)} + O*$	1	0	1	0	0	5
$CO* + O_{2\,(g)} + \bullet \overset{k_6}{\rightarrow} COOO\bullet + *$	0	1	0	0	0	6
$COOO\bullet + * \overset{k_7}{\rightarrow} CO_{2\,(g)} + O* + \bullet$	0	1	0	1	0	7
$O_{2\,(g)} + * \overset{k_8}{\rightarrow} O_2*$	0	0	1	0	1	8
$CO* + O_2* \overset{k_9}{\rightarrow} CO_{2\,(g)} + O* + *$	0	0	0	0	0	9
$O_{2\,(g)} + \bullet \overset{k_{10}}{\rightarrow} O_2\bullet$	0	0	0	1	0	10
$CO* + O_2\bullet \overset{k_{11}}{\rightarrow} CO_{2\,(g)} + O* + \bullet$	0	0	0	0	0	11
$CO* + O_2* \overset{k_{12}}{\rightarrow} COOO* + *$	0	0	1	0	0	12
$CO* + O_2\bullet \overset{k_{13}}{\rightarrow} COOO\bullet + *$	0	0	0	1	0	13
$O_2* + * \overset{k_{14}}{\rightarrow} 2\,O*$	0	0	0	0	1	14

*: Stoichiometric coefficients

2.5.2. Reaction Path B

This mechanism is similar to reaction path A, O_2 is not captured on the catalyst surface but is held as an adsorbed reaction intermediate at the Au-support interface (Steps 1 and 6 in Table 2.1).

2.5.3. Reaction Path C

Reaction pathway is a Langmuir-Hinshelwood-type (L-H-type) mechanism in which the adsorbed CO reacts with adsorbed molecular O_2. The reaction occurs on the sites of pure Au (Steps 1, 3, 5, 8 and 12 in Table 2.1).

2.5.4. Reaction Path D

This path is the same as reaction path C, except for O_2 adsorption as well as intermediate (OO-CO) formation, and decomposition occurs at the perimeter interface rather than at pure Au sites (Steps 1, 3, 7, 10 and 13 in Table 2.1).

2.5.5. Reaction Path E

Although O_2 is not dissociated over Au surfaces, the classical Langmuir-Hinshelwood-type mechanism (proposed for Pt catalysts) involving the reaction between adsorbed CO and adsorbed atomic O (Steps 1, 3, 8 and 14 in Table 2.1) has also been considered for Au catalysts (Davran-Candan, 2011).

3. EXPERIMENTAL WORK

3.1. Materials

3.1.1. Chemicals

The chemicals used for catalyst preparation are listed in Table 3.1.

Table 3.1. Chemicals used in catalyst preparation.

Chemicals	**Formula**	**Grade**	**Source**	**Molecular Weight (g mole^{-1})**
Gold(III) chloride trihydrate	$HAuCl_4.3H_2O$	Extra Pure	Aldrich	393.83
Magnesium nitrate Hexahydrate	$Mg(NO_3)_2.6\ H_2O$	Extra Pure	Merck	256.41
Aluminium oxide	Al_2O_3	Extra Pure	Zeochm EU	101.96
Urea	$CO(NH_2)_2$	Extra Pure	Merck	60.06

3.1.2. Gases and Liquids

All gases and liquids used in this research are listed with their applications and specifications in Table 3.2 and Table 3.3. Oxygen, carbon dioxide and hydrogen were supplied by Birleşik Oksijen Sanayi (BOS), helium was supplied by Linde Company and carbon monoxide was supplied by HABAŞ Company.

Table 3.2. Applications and specifications of the gases used in the kinetic measurements.

Gas	Application	Specification
Carbon monoxide	Reactant, MS calibration	99.0% HABAŞ
Oxygen	Reactant, MS calibration	99.99% BOS
Carbon dioxide	Reactant, MS calibration	99.99% BOS
Hydrogen	Reactant, Reducing agent, MS calibration	99.99% BOS
Helium	Reactant (Inert), MS calibration	99.99% Linde

Table 3.3. Applications and specifications of the liquids used in the kinetic measurements.

Liquid	Application	Specification
Water	Reactant, cleaning	Distilled

3.2. Experimental Set-up

The experimental systems used in this work can be described in three groups:

- Catalyst Preparation System: The loading of Mg promoters on γ-Al_2O_3 support before the addition of Au employed the incipient-to-wetness impregnation method, whereas Au was deposited on the composite MgO/γ-Al_2O_3 support afterwards by using the homogeneous deposition-precipitation (HDP) method.

- Micro-reactor Flow System: The catalytic activity of the catalysts for the selective CO oxidation reaction was tested in a microreactor flow system. The system consists of

mass flow controllers for inlet gases, a liquid pump for water feed, temperature-controlled heated connecting lines and a fixed bed flow reactor located in a vertical furnace coupled with a programmable temperature controller.

- Product Analysis System: The concentrations of the reaction products and feed gases were determined by using an on-line mass spectrometer.

3.2.1. Catalyst Preparation System

Pore volume impregnation method was implemented for the loading of Mg as a promoter onto the γ-Al_2O_3 support. The system used for the preparation of catalyst consists of a Retsch UR1 ultrasonic mixer which provides uniform mixing and contact of the solution with the support, a vacuum pump, a Masterflex computerized-drive peristaltic pump which is used for addition of the solution that will be impregnated, a vacuum flask, a beaker and silicone tubing (Figure 3.1).

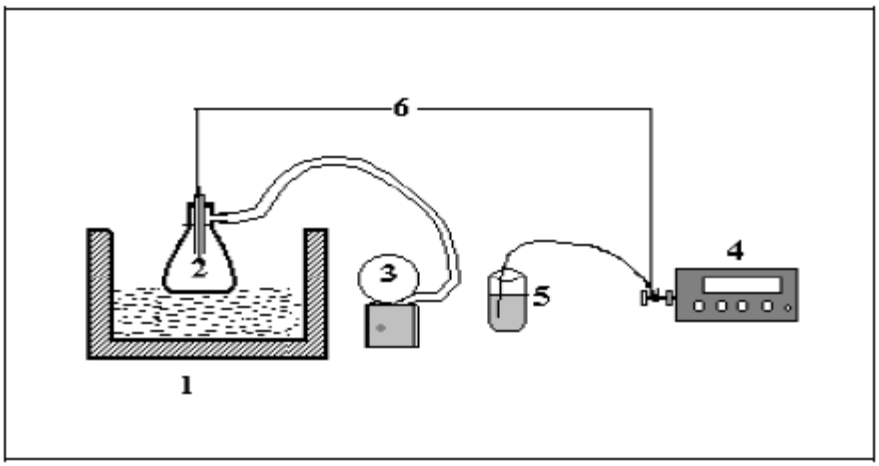

Figure 3.1. The impregnation system: 1.Ultrasonic mixer 2.Büchner flask 3.Vacuum pump 4.Peristaltic pump 5.Beaker 6.Silicone tubing (Başar, 2010).

The deposition of Au over the MgO/γ-Al_2O_3 support was achieved by utilizing the HDP method. The system used in the HDP process is comprised of a stirrer for

homogenous mixing, a heater circulation bath for controlling the temperature of the HDP process, and a pH meter for determination of the alkalinity of the solution (Figure 3.2).

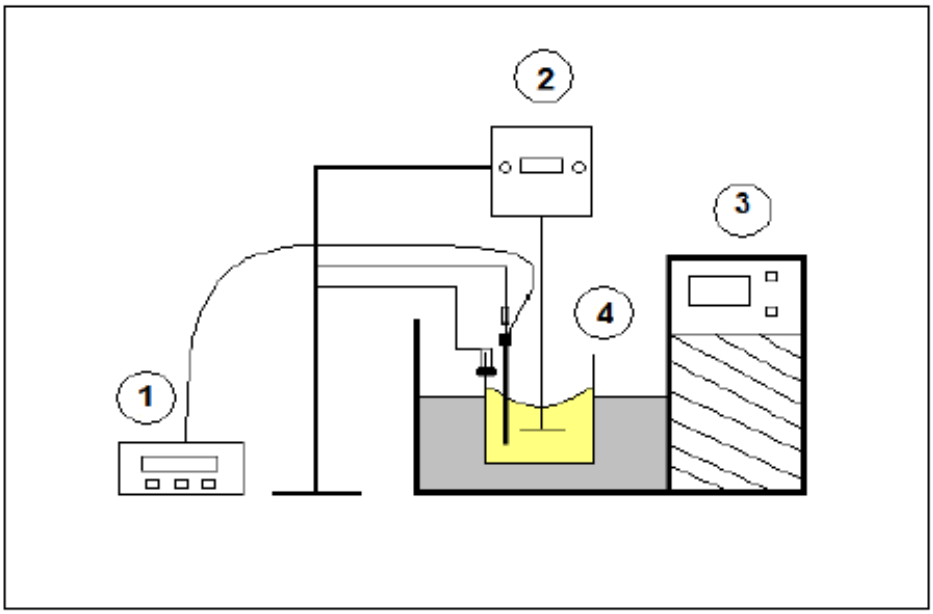

Figure 3.2. The HDP system: 1. pH meter, 2. Stirrer, 3. Heater circulation bath 4. Beaker (Başar, 2010).

3.2.2. Microreactor Flow System

The reactant gases CO, CO_2, He, H_2, and O_2 from pressurized gas cylinders with an optimum pressure of 30 psia were delivered to the microreactor flow system using 1/4″, 1/8″, and 1/16″ OD stainless steel and copper tubing with brass and stainless steel fittings. The flow rates of the gases were controlled by Brooks 5850E mass flow controllers coupled with a 4-Channel Brooks 0154 control panel. All gases used in feed stream were mixed to provide homogeneous mixing before they entered the reactor tube.

The gas mixture was fed to the reaction system including a 4 mm ID x 53 cm stainless steel fixed-bed reactor placed in 2.4 cm ID x 40 cm furnace controlled to 0.5± K with a Eurotherm 2408 programmable temperature controller, shown in Figures 3.3 and 3.4. The K-type sheated thermocouple was placed at the middle of the reactor near the catalyst sample for observing the temperature. The distilled water which was pumped by using an Agilent 1200 Isocratic HPLC pump was heated and kept at approximately 140^{o}C

to enable vaporization of water before entering the system. The gases and water vapor mixture entered the reactor tube, and the exit gas stream from the reactor was passed through a cold trap consisting of an ice box and coiled tubing, which was used to increase contact time of gases in the trap.

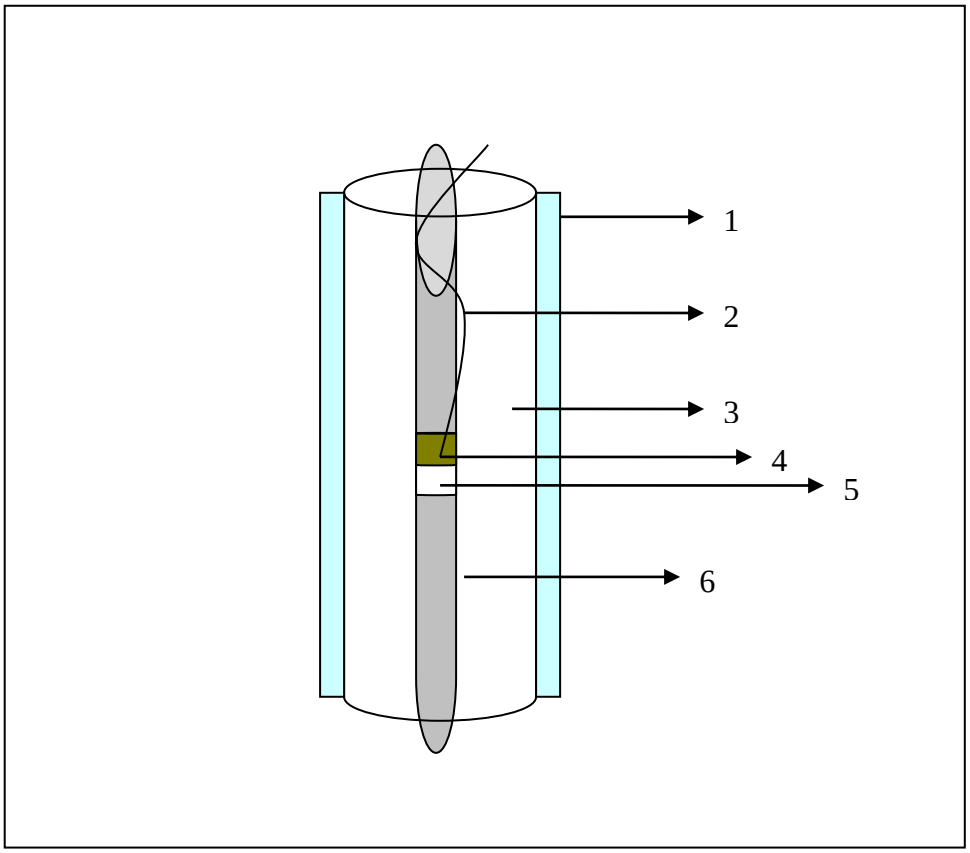

Figure 3.3. Reactor and furnace system: 1.Ceramic wool insulation 2.Thermocouple 3.Furnace 4.Catalyst 5.Catalyst bed 6. Reactor (Tezcanlı, 2008).

3.2.3. Product Analysis System

The product stream and the feed gas were sent and analyzed by using an on-line Hiden Hal 210 mass spectrometer connected to a personal computer employing MASsoft software. The entire microflow reaction system is presented in Figure 3.4.

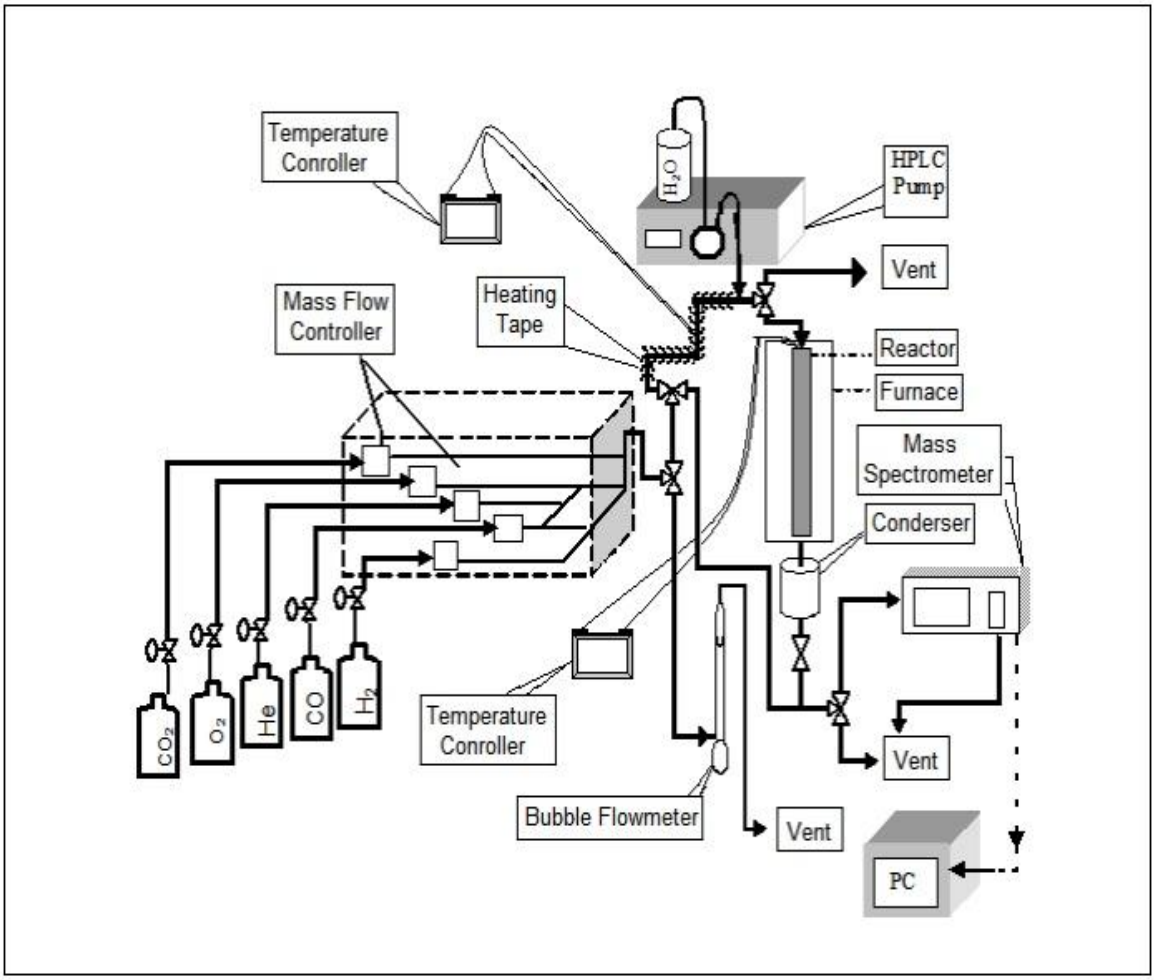

Figure 3.4. The microreactor flow and product analysis system (Tezcanlı, 2008).

3.3. Catalyst Preparation

In this study, preparation of the catalyst selected involves two steps, namely, incipient-to-wetness impregnation followed by homogeneous-deposition-precipitation. The first step is loading of the Mg promoter on γ-Al_2O_3 support by incipient-to-wetness impregnation method, (Figure 3.1) to prepare the Mg-promoted γ-Al_2O_3 support. The promoter content of the MgO/γ-Al_2O_3 composite support was selected as 1.25wt% of the total catalyst weight. The experimental set-up in Figure 3.2 was used to obtain the nanosized gold particles over the MgO/γ-Al_2O_3 composite support by homogeneous-deposition-precipitation, using urea as the precipitating agent.

The γ-Al_2O_3 support was crushed and sieved into 45-60 mesh size (344-255 μm). For removing the air trapped in the pores, a measured amount of support was placed in a vacuum flask and kept under the vacuum for 30 min by mixing the catalyst in a Retsch UR 1 ultrasonic mixer. Before impregnation of the Mg solution over γ-Al_2O_3, the metal salt was first dissolved in 1.21 ml of water per gram of alumina support, which is the amount of water needed for wetting one gram of 344-255 μm γ-Al_2O_3 particles. Addition of the Mg precursor solution to the vacuum flask was achieved by a Master flex computerized-drive peristaltic pump at a rate of 0.5 ml/min via silicon tubing. After adding Mg precursor solution, the slurry was kept under vacuum for 90 min in the ultrasonic mixer in order to obtain a uniform dispersion of the active component. The slurry was then dried in an electrical oven at 80^oC for at least 16 hours to remove water from the composite support.

The calcination operation was performed just before the loading of Au in order to convert the salt or hydroxide form of the active components into oxides by reacting with air at high temperature for enhancing the surface and mechanical properties of the catalysts. The MgO/γ-Al_2O_3 support was calcined in a flow of air at 400^oC with a ramping rate of 5^oC/min and kept at this temperature for 2 hours.

The addition of 1 wt% Au over MgO/γ-Al_2O_3 was achieved by homogeneous deposition precipitation using urea as precipitating agent (Grisel and Nieuwenhuys, 2001). An aqueous solution of $HAuCl_4.3H_2O$ was used as Au precursor. 25 ml of an 8.12 x 10^{-3} M $HAuCl_4.3H_2O$ solution was added to the MgO/γ-Al_2O_3 support suspended in 80 ml demineralized water. 100 ml of a solution with 0.84 M excess urea was added in order to gradually increase pH. The suspension was vigorously stirred and heated to 70^oC in order to gradually decompose the urea and achieve pH increase at 7-8 levels enabling the precipitation of Au nanoparticles on the MgO/γ-Al_2O_3 support. The implementation of this procedure was accomplished with minimal exposure to light in order to avoid possible photochemical reactions of the Au precursors. The suspension was then cooled down, suction filtered, washed with de-ionized water and dried overnight at 100^oC.

3.4. Kinetic Measurements

The kinetic experiments were carried out in the microreactor flow system, presented in Figure 3.4, using Au-based catalysts, which were first reduced in a stream of 50% H_2 in He for 30 min at 300°C before reaction, then kept under a stream of He until the reaction test was performed. For all Au-based catalysts, the reduction procedure is given for in Table 3.4.

Table 3.4. Reduction program for Au-based catalyst.

Segments	**Starting and End Temperatures**	**Segment Gas**
First Segment	Heating from 25˚C to 300˚C with a heating rate of 10ºC/min	H_2 with flow rate of 50 ml/min
Second Segment (Reduction)	Keeping constant at 300˚C for 30 min	H_2 with flow rate of 50 ml/min
Third Segment	Cooling down to reaction temperature	He with flow rate of 50 ml/min

After reduction, all the kinetic measurements listed in Tables 3.5-3.8 were made by employing the $Au/MgO/Al_2O_3$ catalyst under a total flow of 150 ml/min at a reaction temperature of 130°C and atmospheric pressure. In order to limit the conversions to low values, the catalyst samples were diluted with γ-Al_2O_3, which is not active for selective CO oxidation under the reaction conditions, keeping the total bed weight constant at 250 mg. All reaction conditions are presented in Table 3.5, Table 3.6, Table 3.7, and Table 3.8. The ratio of catalyst bed lenght to catalyst particle size (L/d_p) kept at 70-80 in order to ensure plug flow behavior in the reactor, where the L and d_p values are $2.5x10^{-2}$ m and $3.4x10^{-4}$ m, respectively.

Table 3.5. The reaction conditions for 1wt%Au-1.25wt% MgO/Al_2O_3 catalyst at 130°C.

Exp. No	**Total Flow ($ml.min^{-1}$)**	**Weight of Catalyst (mg)**	**Feed Composition (%) with He as Balance**	
			CO	**O_2**
1	150	20	8	4
2	150	40	8	4
3	150	60	8	4
4	150	80	8	4
5	150	100	8	4
6	150	20	6	4
7	150	40	6	4
8	150	20	6	6
9	150	40	6	6
10	150	20	6	3
11	150	40	6	3
12	150	60	6	3
13	150	80	6	3
14	150	100	6	3
15	150	20	4	2
16	150	40	4	2
17	150	60	4	2
18	150	80	4	2
19	150	100	4	2
20	150	20	3	6
21	150	20	3	3
22	150	40	3	3
23	150	20	3	2.25
24	150	40	3	2.25
25	150	20	3	1.5
26	150	40	3	1.5
27	150	60	3	1.5
28	150	80	3	1.5
29	150	100	3	1.5
30	250	20	2	5
31	150	20	2	1
32	150	40	2	1
33	150	60	2	1
34	150	80	2	1
35	150	100	2	1

Table 3.6. The reaction conditions for 1wt%Au-1.25wt% MgO/Al_2O_3 catalyst in the presence of H_2 at 130°C.

Exp. No	**Total Flow ($ml.min^{-1}$)**	**Weight of Catalyst (mg)**	**Feed Composition (%) with He as Balance**		
			CO	**O_2**	**H_2**
1	150	20	4	2	4
2	150	40	4	2	4
3	150	60	4	2	4
4	150	20	4	2	10
5	150	40	4	2	10
6	150	60	4	2	10
7	150	20	4	2	20
8	150	40	4	2	20
9	150	60	4	2	20

Table 3.7. The reaction conditions for 1wt%Au-1.25wt% MgO/Al_2O_3 catalyst in the presence of CO_2 at 130°C.

Exp. No	**Total Flow ($ml.min^{-1}$)**	**Weight of Catalyst (mg)**	**Feed Composition (%) with He as Balance**		
			CO	**O_2**	**CO_2**
1	150	20	6	3	2
2	150	20	6	3	4
3	150	20	6	3	6

Table 3.8. The reaction conditions for 1wt%Au-1.25wt% MgO/Al_2O_3 catalyst in the presence of H_2O at 130°C.

Exp. No	**Total Flow ($ml.min^{-1}$)**	**Weight of Catalyst (mg)**	**Feed Composition (%) with He as Balance**			
			CO	**O_2**	**H_2**	**H_2O**
1	150	20	4	2	20	2
2	150	20	4	2	20	4
3	150	20	4	2	20	6

4. RESULTS AND DISCUSSION

4.1. Introduction

In the present work, low-temperature CO oxidation was investigated over 1wt%Au-1.25wt%MgO/Al_2O_3 at 130°C and atmospheric pressure. Catalytic activity tests and kinetic experiments were performed at stoichiometric and non-stoichiometric CO/O_2 ratios, in the absence of H_2, CO_2 or H_2O in the feed stream. Subsequently, the effects of H_2, CO_2 and/or H_2O addition to the feed were also studied. CO conversion (X_{CO}), and the amount of water vapor in the feed were calculated by using the following relationships:

$$CO\ conversion\ (\%) = \frac{[CO]_{in} - [CO]_{out}}{[CO]_{in}} x100 \tag{4.1}$$

$$V_{Steam(H_2O)} = \frac{V_{liquid(H_2O)}\ x\ \rho_{H_2O}\ x\ R\ x\ T}{MW_{H_2O}\ x\ P} \tag{4.2}$$

where ρ=1000 $g.L^{-1}$; P=1 atm; R=0.082 $L.atm.mol^{-1}.K^{-1}$; T=298 K and MW_{H2O}=18 $g.mol^{-1}$.

In the kinetic experiments, the catalyst mass based initial reaction rates $(-r_{CO})$ were evaluated from the conversion versus residence time $\left(W_{cat}/F_{CO_{in}}\right)$ data as follows;

$$(-r_{CO}) = \frac{dx_{CO}}{d\left(W_{cat}/F_{CO_{in}}\right)} \tag{4.3}$$

where x_{CO} is carbon monoxide conversion, $F_{CO_{in}}$ is carbon monoxide flow rate in the feed in $ml.min^{-1}$ converted to $mol.h^{-1}$, W_{cat} is catalyst weight in g and $(-r_{CO})$ is the reaction rate in $mol.g^{-1}.h^{-1}$. Carbon monoxide consumption rates were calculated from the slopes of the x_{CO} vs. $\left(W_{cat}/F_{CO_{in}}\right)$ curves at the initial rates region or, at higher contact times, from the slopes of the tangents to the curves at different W/F_{CO} values.

4.2. Preliminary Experiments

Prior to any catalytic activity or kinetic data collection, preliminary experiments were conducted over the 0.5wt%Au/Al_2O_3 catalyst using different total flow rates, namely 100, 120 and 150 ml/min, for a fixed feed composition of 1%CO+1%O_2+60%H_2 and different weights of catalyst proportional to total flow rate, 10, 12 and 15 mg, and 20, 24 and 30 mg, in order to determine the mass transfer effect in the 90-130^oC temperature range. The CO conversions obtained are presented in Table 4.1. and Table 4.2, while the CO conversion versus total flow rate data at three different temperatures are plotted in Figure 4.1. and Figure 4.2. After investigating the interaction between chemical and physical rate phenomena in the fixed-bed micro-reactor at constant contact time, and ensuring the total absence of transport effects, it was decided that the reaction-controlled regime was reached after 120 ml/min; therefore, a total flow rate 150 ml/min was used in all subsequent activity tests and kinetic experiments.

Table 4.1. The CO conversions at different total flow rates and temperatures in the presence of H_2 over 0.5wt%Au/Al_2O_3 for 1%CO + 1%O_2 + 60%H_2 feed.

	F=100 ml/min	**F=120 ml/min**	**F=150 ml/min**
T=90^oC	0.11	0.13	0.11
T=110^oC	0.20	0.22	0.22
T=130^oC	0.20	0.21	0.20

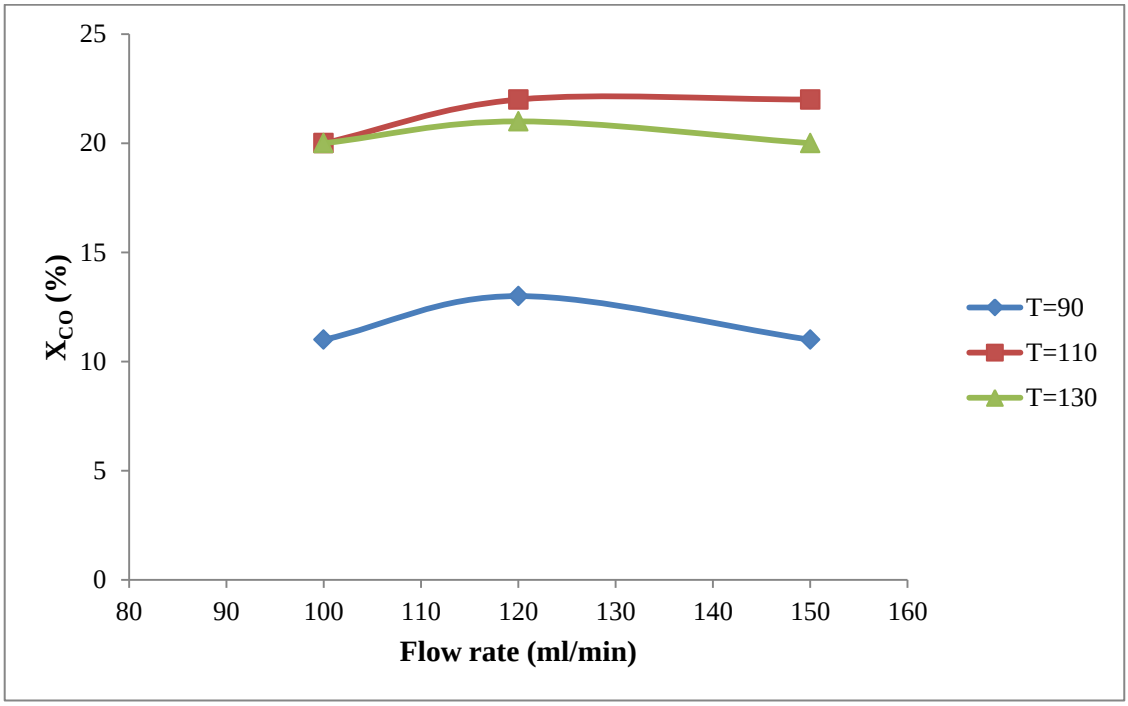

Figure 4.1. Effect of the total flow rate on the conversion at different temperatures in the presence of H_2 over 0.5wt%Au/Al_2O_3 for 1%CO + 1%O_2 + 60%H_2 feed.

Table 4.2. The CO conversions at different total flow rates and temperatures in the absence of H_2 over 0.5wt%Au/Al_2O_3 for 1%CO +1%O_2 feed.

	F=100 ml/min	**F=120 ml/min**	**F=150 ml/min**
T=90°C	0.035	0.038	0.040
T=110°C	0.051	0.049	0.070
T=130°C	0.101	0.086	0.107

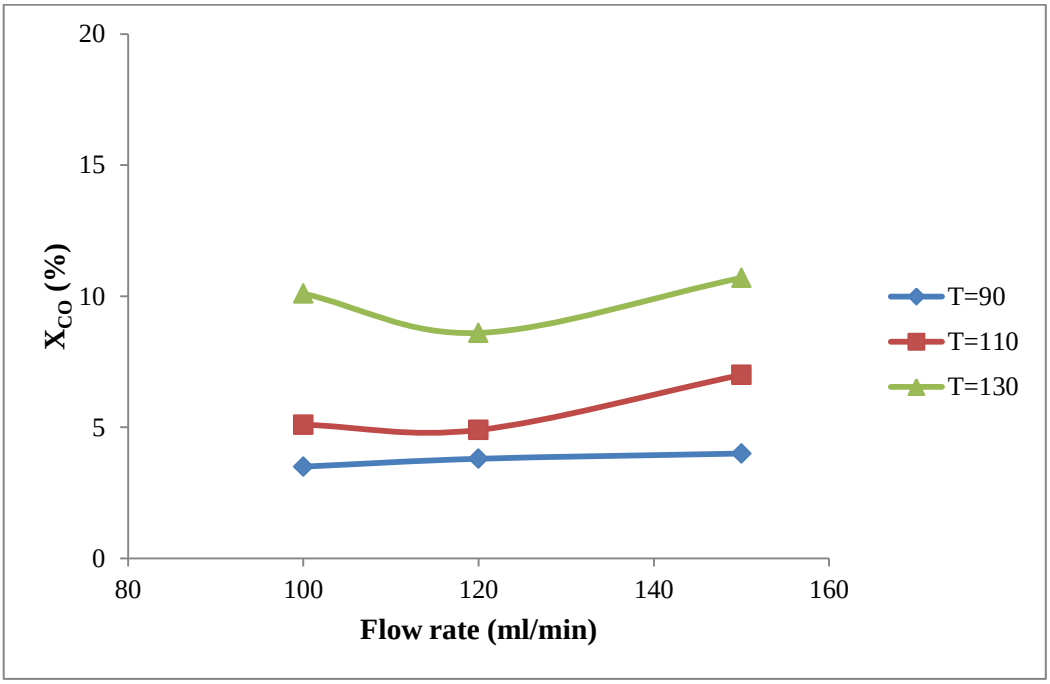

Figure 4.2. Effect of the total flow rate on the conversion at different temperatures in the absence of H_2 over 0.5wt%Au/Al_2O_3 for 1%CO +1%O_2 feed.

4.3. Kinetic Study of Carbon Monoxide Oxidation

The reaction conditions used in the kinetic experiments for examining the effect of the CO/O_2 ratio, H_2 concentration, and the presence of CO_2 and H_2O on the kinetics of carbon monoxide oxidation over the 1wt%Au-1.25wt%MgO/Al_2O_3 catalyst were presented in Tables 3.5-3.8 of Section 3.4. The kinetics of low-temperature CO oxidation over the 1wt% Au-1.25wt%MgO/Al_2O_3 catalyst was studied in a fairly wide range of CO (2-8 mol per cent) and O_2 (1-6 mol per cent) concentrations in the initial rates region, and at higher contact times, at constant reaction temperature of 130^{o}C. The dependence of CO oxidation rates on CO and O_2 partial pressures was examined. Measurements for the determination of reaction orders with respect to CO and O_2 were taken by varying both the catalyst weight and the CO and O_2 concentrations in the feed (Table 4.3), the data obtained were then used for the kinetic calculations.

Table 4.3. Kinetic data on CO oxidation over 1wt%Au-1.25wt% MgO/Al_2O_3 at 130°C.

Exp. No	W (mg)	Total Flow ($ml.min^{-1}$)	W/Fco ($g.h.mol^{-1}$)	CO (mol%)	O_2 (mol%)	Fractional conversion Xco
1	20	150	0.67	8	4	0.15
2	40	150	1.35	8	4	0.27
3	60	150	2.03	8	4	0.38
4	80	150	2.71	8	4	0.53
5	100	150	3.39	8	4	0.62
6	20	150	0.90	6	6	0.22
7	40	150	1.81	6	6	0.50
8	20	150	0.90	6	4	0.21
9	40	150	1.81	6	4	0.43
10	20	150	0.90	6	3	0.13
11	40	150	1.81	6	3	0.26
12	60	150	2.71	6	3	0.41
13	80	150	3.62	6	3	0.51
14	100	150	4.52	6	3	0.60
15	20	150	1.35	4	2	0.16
16	40	150	2.71	4	2	0.30
17	60	150	4.07	4	2	0.44
18	80	150	5.43	4	2	0.54
19	100	150	6.79	4	2	0.56
20	20	150	1.81	3	6	0.23
21	20	150	1.81	3	3	0.26
22	40	150	3.62	3	3	0.46
23	20	150	1.81	3	2.25	0.21
24	40	150	3.62	3	2.25	0.43
25	20	150	1.81	3	1.5	0.16
26	40	150	3.62	3	1.5	0.30
27	60	150	5.43	3	1.5	0.44
28	80	150	7.24	3	1.5	0.55
29	100	150	9.05	3	1.5	0.60
30	20	150	2.71	2	5	0.26
31	20	150	2.71	2	1	0.16
32	40	150	5.43	2	1	0.29
33	60	150	8.14	2	1	0.42
34	80	150	10.86	2	1	0.46
35	100	150	13.58	2	1	0.56

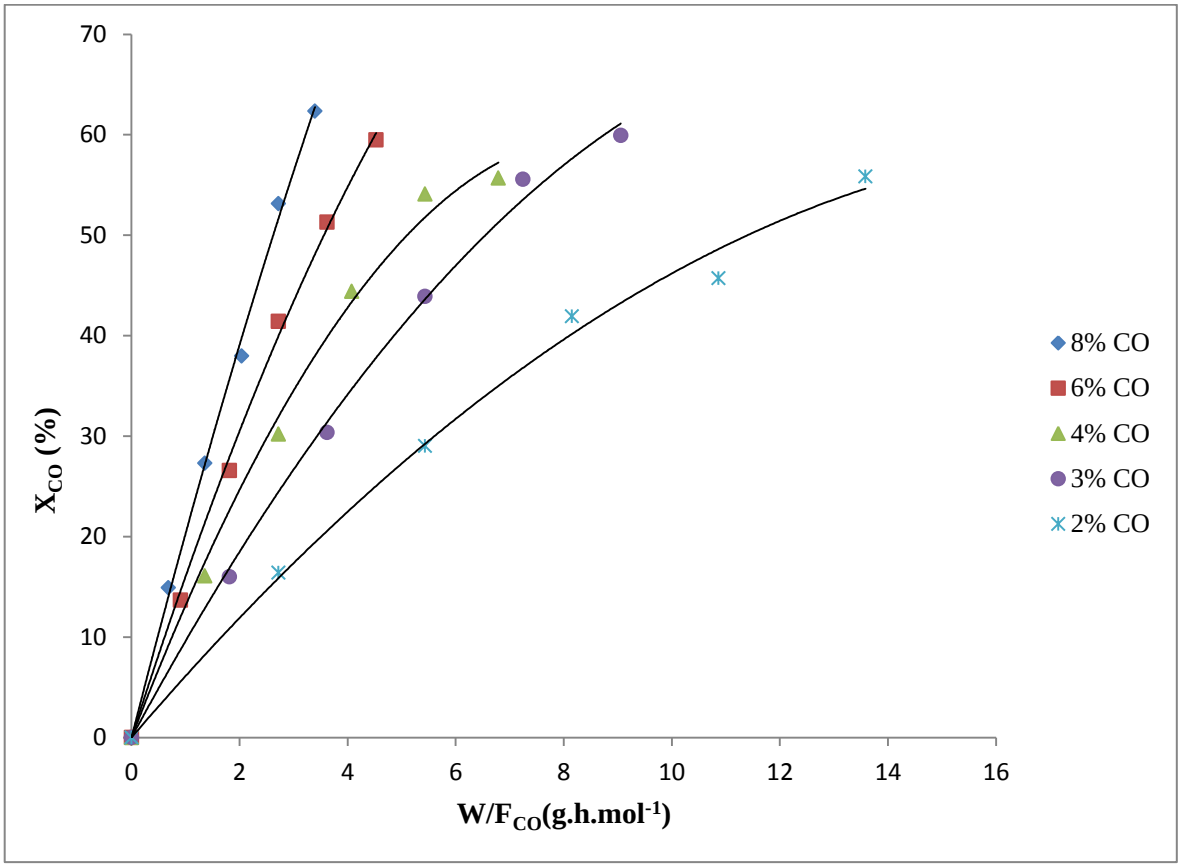

Figure 4.3. Conversion of carbon monoxide as a function of space time at various initial CO concentrations over 1wt% Au-1.25wt% MgO/Al_2O_3 at 130°C and O_2/CO = 0.50.

The fractional CO conversions (x_{CO}) obtained at various initial CO concentrations using O_2/CO = 0.50 are plotted in Figure 4.3 as a function of space time. Increasing $(W_{cat}/F_{CO_{in}})$ values resulted in the enhancement of CO conversion, as expected in CO oxidation in the absence of H_2 in the feed. At all initial feed concentrations, CO conversion first increases rather sharply with increasing space time and later slows down gradually.

4.3.1. Power Law Modeling of the Kinetic Data

The experimental data presented in Table 4.3 were used to calculate the reaction rates in Table 4.4 and then fitted to a power function rate expression of the following form in order to determine the model parameters for carbon monoxide oxidation:

$$(-r_{CO}) = k(P_{CO})^{\alpha}\left(P_{O_2}\right)^{\beta} \qquad (4.4)$$

The resulting rate versus partial pressure data given in Table 4.4 were processed using nonlinear regression analysis according to the Levenberg-Marquardt algorithm in the computer software MATLAB environment in order to estimate the parameters, *k*, α and β of Equation 4.4.

The Levenberg-Marquardt algorithm is an iterative technique that locates the minimum of a function that is expressed as the sum of squares of nonlinear functions (Equation 4.5). The sum of the squared differences of the measured reaction rates, $(-r)_m$, and the calculated reaction rates, $(-r)_c$, for N experiments and p parameter values is defined as variance of experimental error given by the following equation:

$$\sigma^2 = \sum_{i=1}^{n} \frac{[(-r)_{im} - (-r)_{ic}]^2}{(N-p)} \rightarrow Minimum \qquad (4.5)$$

Table 4.4. Partial pressures of CO and O_2 and calculated initial rates of CO oxidation over 1wt%Au-1.25wt%MgO/Al_2O_3 at 130^{o}C.

Experiment run	**Partial Pressures (atm)**		$(-r_{co})$ **(mol.g^{-1}.h^{-1})**
	CO	**O_2**	
1	0.08	0.04	0.2198
2	0.06	0.06	0.2447
3	0.06	0.04	0.2340
4	0.06	0.03	0.1509
5	0.04	0.02	0.1185
6	0.03	0.06	0.1282
7	0.03	0.03	0.1461
8	0.03	0.0225	0.1174
9	0.03	0.015	0.0883
10	0.02	0.05	0.0969
11	0.02	0.01	0.0604

The reaction orders with respect to CO (α) and O_2 (β) were determined as 0.61 and 0.36, respectively. The reaction rate constant, *k*, was found as 3.55 $mol.g^{-1}.h^{-1}.atm^{-1}$. Consequently, the power-function rate equation for low-temperature CO oxidation over 1wt%Au-1.25wt%MgO/Al_2O_3 at 130°C in the initial rate region can be given as:

$$(-r_{CO}) = 3.55(P_{CO})^{0.61}\left(P_{O_2}\right)^{0.36} \tag{4.6}$$

The variance of experimental error is found to be 0.0042 for this rate expression. The fit between experimentally measured and model predicted rates is reasonably good with a mean squared error of 0.92; this is demonstrated in Figure 4.4 which takes into account all individual rates used in the non-linear regression analysis.

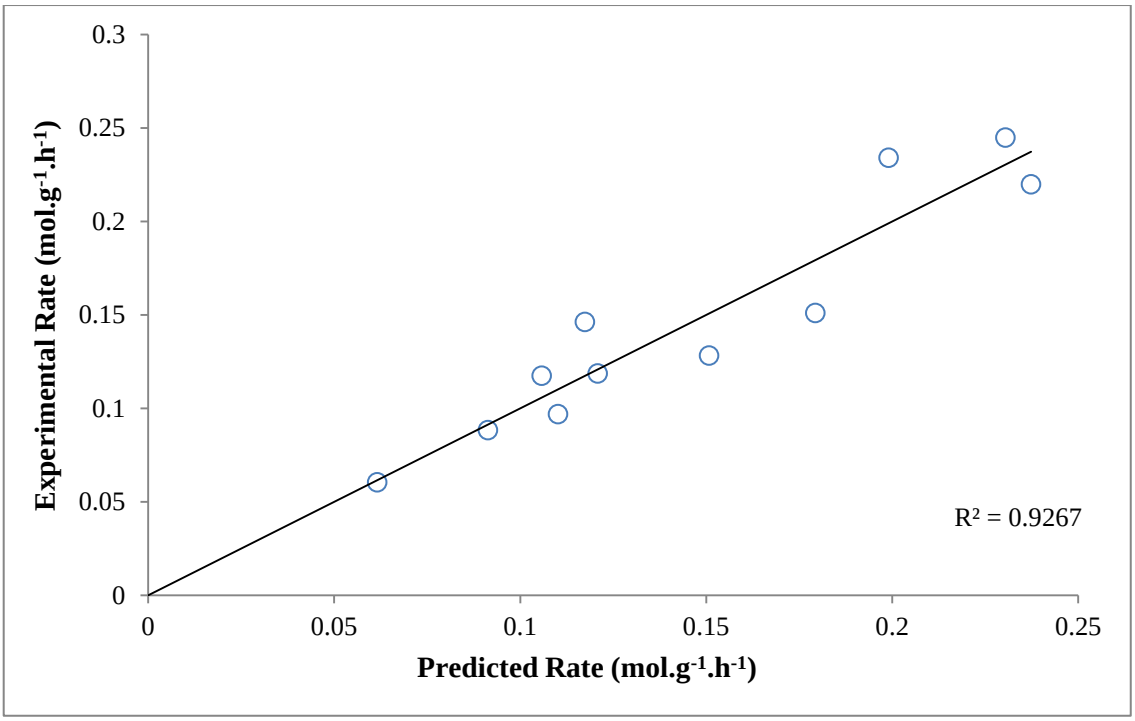

Figure 4.4. Experimental rates versus predicted rates (power law model) for low-temperature CO oxidation over 1wt%Au-1.25wt%MgO/Al_2O_3.

Schubert *et al.* (1999) reported that the kinetics of CO oxidation over Au/Fe_2O_3 catalyst at 80°C give reaction orders with respect to CO and O_2 of 0.55 and 0.23,

respectively. The reaction orders were found to be 0.19 for CO and 0.18 for O_2 using a CeO_2-supported gold catalyst at 303 K (Aguilar-Guerrero *et al.*, 2008). The results of parameter estimation for CO oxidation over 1.5% Au-1% Pt/ZnO at 573 K showed that the reaction orders with respect to CO and O_2 were 0.68 and 0.34, respectively (Wang *et al.*, 2006). The kinetic study of CO oxidation performed over a Au/TiO_2 catalyst at 80^oC indicated reaction orders with respect to CO and O_2 of 0.34 and 0.32, respectively (Schumacher *et al.*, 2004). In the present study, the reaction orders with respect to CO and O_2 were found to be 0.61 and 0.36, respectively, implying that the CO coverage is significantly below saturation while that of O_2 is comparatively higher. The reaction orders obtained in the kinetic studies reported in the literature are compared in Table 4.5.

Table 4.5. Comparison of reaction orders obtained with respect to CO (α) and O_2 (β) over supported gold catalysts.

Catalyst	**α**	**β**	**Reference**
Au/Fe_2O_3	0.55	0.23	Schubert *et al.*, 1999
Au/CeO_2	0.19	0.18	Aguilar-Guerrero *et al.*, 2008
Au-Pt/ZnO	0.68	0.34	Wang *et al.*, 2006
Au/TiO_2	0.34	0.32	Schumacher *et al.*, 2004
$Au/MgO/Al_2O_3$	0.61	0.36	Present work

4.3.2. Langmuir-Hinshelwood-Hougen-Watson Kinetics

Determination of heterogeneous catalytic reaction mechanisms with surface reaction as the rate-limiting step is termed as the Langmuir-Hinshelwood approach, since it is derived from ideas proposed by Hinshelwood based on Langmuir's quantitative treatment

of chemical adsorption. This approach was later generalized by Hougen and Watson to cover all possible rate-limiting steps in a heterogeneous catalytic reaction mechanism. An LHHW equation can be derived by first assuming a sequence of elementary steps in the reaction, among which molecular or atomic adsorption, single or dual site reaction are considered. Rate laws are then written for the individual steps assuming all the steps are reversible. Finally, a rate limiting step is postulated, and steps that are not rate-limiting are used to eliminate all coverage-dependent terms.

In general, bimolecular surface reactions have more significance in the catalytic action on solids than unimolecular reactions. If reactants are competitively adsorbed on equivalent surface sites, the reaction rate takes the form of Equation (4.7). If reactants are separately adsorbed on different types of surface sites, they do not displace each other from the surface, and the reaction rate takes the form of Equation (4.8) (Fogler, 2006). In both cases dual-site mechanisms, i.e the use of two sites per reaction cycle, are involved.

$$(-r_{CO}) = \frac{kP_{CO}P_{O_2}}{\left(1 + K_1P_{CO} + K_2P_{O_2}\right)^2} \tag{4.7}$$

$$(-r_{CO}) = \frac{kP_{CO}P_{O_2}}{(1 + K_1P_{CO})\left(1 + K_2P_{O_2}\right)} \tag{4.8}$$

In this study, Langmuir-Hinshelwood rate expressions with dual site mechanisms involving separate or competitive adsorption of CO and O_2 were used to fit experimental data. Rate parameters were estimated with nonlinear least-squares analysis according to the Marquardt-Levenberg algoritm using MATLAB computer software. The models used and the values of the kinetic parameters obtained for these models are presented in Table 4.6.

Table 4.6. Langmuir-Hinshelwood rate expressions analyzed for CO oxidation over 1wt%Au-1.25wt%MgO/Al_2O_3 at 130^{o}C.

Model No	**Rate Equations**	**Rate parameters**	**σ^2 $(mol.g^{-1}.h^{-1})^2$**
1	$(-r_{CO}) = \frac{kP_{CO}P_{O_2}}{(1+K_1P_{CO})(1+K_2P_{O_2})}$	k=527 $mol.g^{-1}.h^{-1}.atm^{-1}$ K_1=16.53 atm^{-1} K_2=53.11 atm^{-1}	0.0038
2	$(-r_{CO}) = \frac{kP_{CO}P_{O_2}}{(1+K_1P_{CO}+K_2P_{O_2})^2}$	k=551 $mol.g^{-1}.h^{-1}.atm^{-1}$ K_1=12.20 atm^{-1} K_2=20.17 atm^{-1}	0.0031

Rate values predicted by Model I and Model II are plotted versus experimental rate values in Figure 4.5 and Figure 4.6, respectively, together with the corresponding mean squared errors. Statistical fit of both models to the experimental data is reasonably good, indicating that two sites are involved per reaction cycle. Although kinetic studies are not sufficient for drawing mechanistic conclusions, good statistical fit of data to models that consider either separate or competitive adsorption of CO and O_2 indicates the involvement of MgO and that the surface reaction may be occurring between CO and oxygen adsorbed on adjacent Au sites or at their peripheries.

It has been reported that the closeness of the reaction orders for CO and O_2 implies competetive adsorption on gold sites (Aguilar-Guerrero *et al.*, 2008). The positive reaction order in CO indicates that, unlike Pt catalysts, CO oxidation over Au catalysts is not hindered by strong CO adsorption (Schubert *et al.*, 1999).

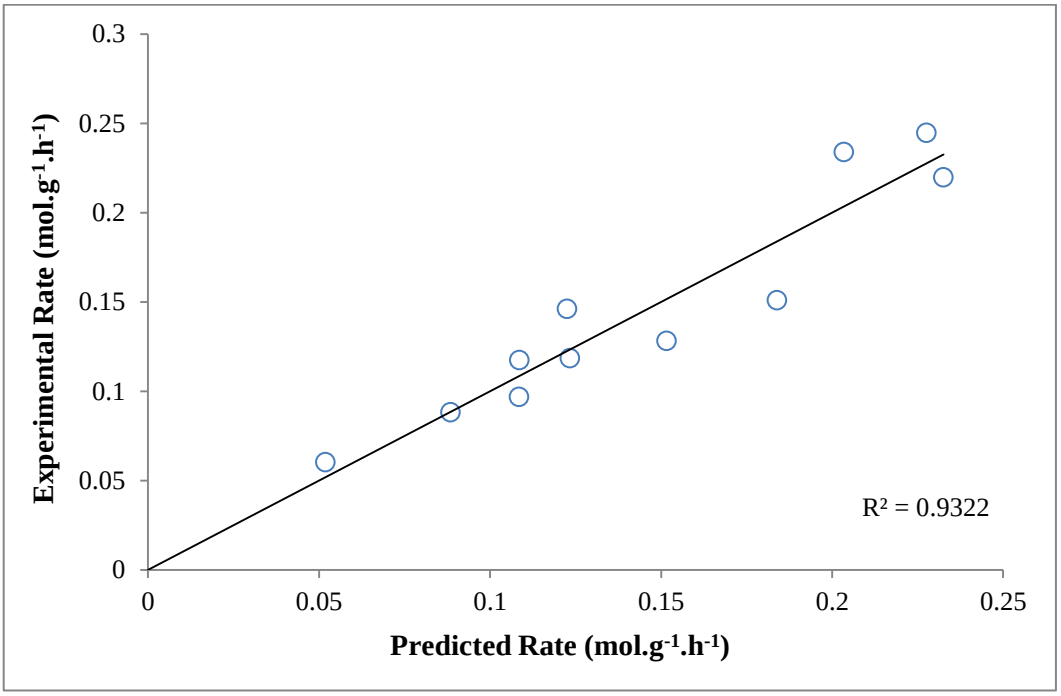

Figure 4.5. Experimental rates versus predicted rates (Model I) of low-temperature CO oxidation over 1wt%Au-1.25wt%MgO/Al_2O_3 at 130^{o}C.

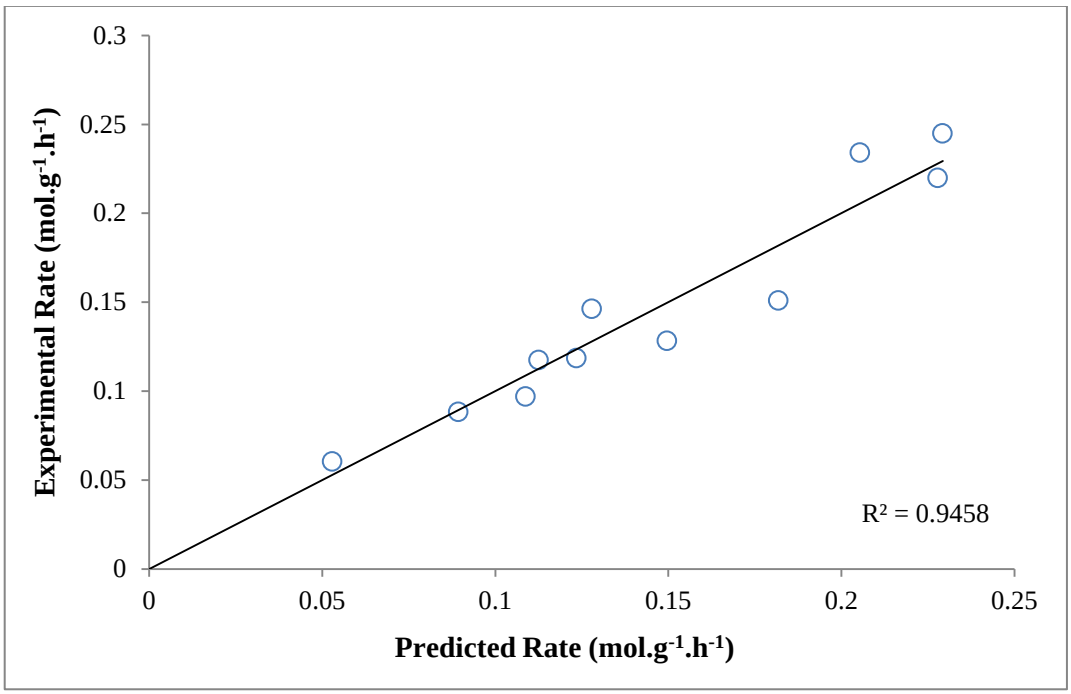

Figure 4.6. Experimental rates versus predicted rates (Model II) of low-temperature CO oxidation over 1wt%Au-1.25wt%MgO/Al_2O_3 at 130^{o}C.

4.4. The Effect of H_2 on Low-Temperature CO Oxidation

Effect of H_2 on CO conversion over 1wt%Au-1.25wt%MgO/Al_2O_3 was also studied at 130^{o}C in a feed with 4%CO and 2%O_2, using different amounts of catalyst weight, 20, 40 and 60 mg, specifically in the initial rates region, and varying inlet H_2 concentration from 4 to 20% by partially replacing the inert He. The corresponding data are presented in Table 4.7 and plotted in Figure 4.7. A comparison of the experimental results obtained in the absence and presence of H_2 in the feed shows that H_2 has an enhancement effect on CO oxidation which gradually diminishes as H_2 concentration is increased.

Table 4.7. CO conversions at different space times in the presence of H_2 in the feed over 1wt%Au-1.25wt%MgO/Al_2O_3 at 130°C.

Exp. No	**Total Flow (ml.min^{-1})**	**W/F_{CO} (g.h.mol^{-1})**	**Weight of Catalyst (mg)**	**Feed Composition (mol%) with He as Balance**			**X_{CO}**
				CO	**O_2**	**H_2**	
1	150	1.35	20	4	2	4	0.64
2	150	2.71	40	4	2	4	0.62
3	150	4.07	60	4	2	4	0.58
4	150	1.35	20	4	2	10	0.61
5	150	2.71	40	4	2	10	0.50
6	150	4.07	60	4	2	10	0.46
7	150	1.35	20	4	2	20	0.38
8	150	2.71	40	4	2	20	0.34
9	150	4.07	60	4	2	20	0.32
15*	150	1.35	20	4	2	0	0.16
16*	150	2.71	40	4	2	0	0.30
17*	150	4.07	60	4	2	0	0.44

*: Data from Table 4.3.

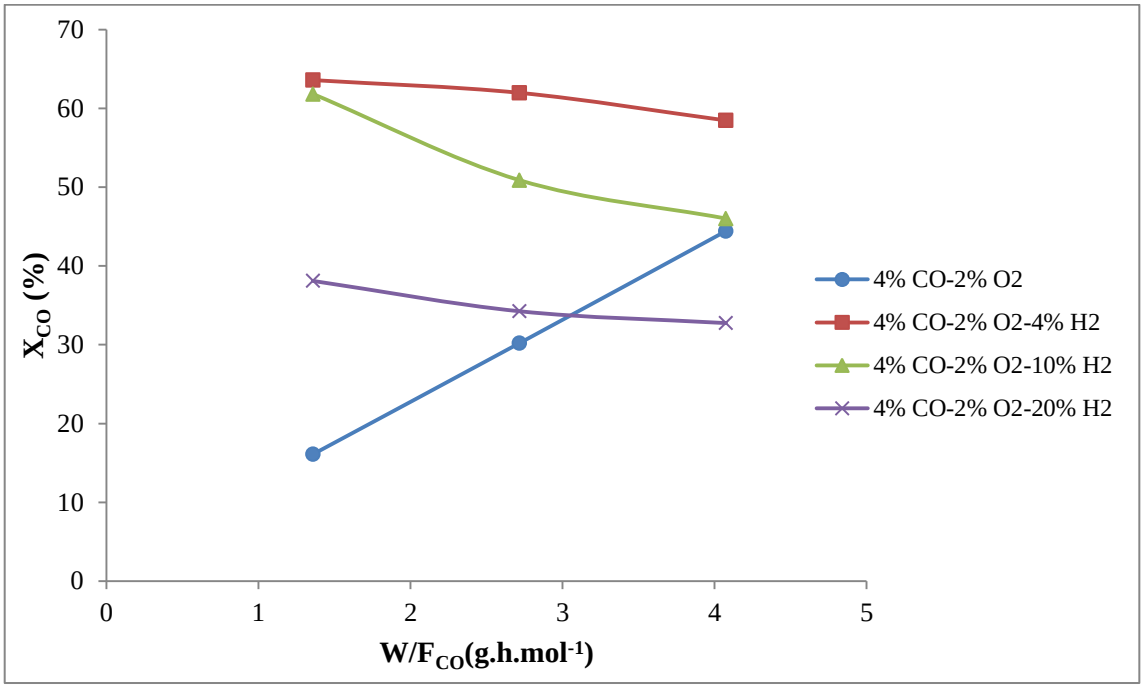

Figure 4.7. Effect of H_2 on CO conversion over 1wt%Au-1.25wt%MgO/Al_2O_3 at 130°C.

The experimental results plotted in Figure 4.7 also point out that the presence of H_2 in the feed results in an increase in the CO conversion. The H_2-induced enhancement in CO conversions over 1wt%Au-1.25wt%MgO/Al_2O_3 varies from four to two fold at H_2 concentrations between 4-20 mol% at W/F_{CO} = 1.35 g.h.mol^{-1} . The lowest amount of feed H_2 (4 mol%) in the feed leads to the highest CO conversion levels, but increasing the H_2 concentration to 10 mol% and 20 mol% reduces the CO conversion levels, although these conversions are still higher than the CO conversions obtained in the absence of H_2 at low space times. For example, on the 40 mg catalyst (W/F_{CO} = 2.71g.h.mol^{-1}), CO conversion is 30% in the absence of hydrogen. Addition of 4%H_2 to the feed boosts CO conversion up to 62%. When the H_2 in the feed is increased to 10 mol%, CO conversion decreases to 50%, and with further increase in H_2 to 20 mol%, CO conversion decreases down to 32%. The reason of this is attributed to the strong adsorption of CO on the Au surfaces where H_2 adsorption and competing reactions may also occur because of the high concentration of H_2 in the reactants stream.

The effect of H_2 on the oxidation of CO was examined over Pt catalyst in the absence of water vapor at 170°C. It was found that H_2 accelerates CO conversion (Muraki *et al.*, 1991). The presence of H_2 has a favourable effect on the oxidation of CO, either by

strongly accelerating the reaction or by preventing the catalyst deactivation (Quinet *et al.*, 2008a). Higher hydrogen concentrations cause competition between CO and H_2 oxidations at lower temperatures. It is proposed that hydrogen reacts with oxygen to yield highly oxidizing intermediates that selectively react with CO to produce water. Experimental results they reported indicate that the rate of CO oxidation over Au/Al_2O_3 was strongly enhanced by the introduction of even a very small amount of hydrogen (0.25%) into the reactant mixture. In the presence of both oxygen and hydrogen, highly active –OOH species are formed on the surface of the gold catalyst (Quinet *et al.*, 2008b).

The mechanisms of CO oxidation and hence the effect of H_2 in the feed depend on the nature of active metals, promoters and supports used in catalyst formulation. The H_2-induced enhancement in CO oxidation rates over 1wt%Pt-0.25wt%SnO_x/AC3 was found to be nearly ten fold at H_2 concentrations above 30 mol% (Soyal-Baltacıoğlu *et al*. 2007). Possible reasons for this enhancement were proposed as the interaction of H_2 with oxygen-bearing surface groups of the HNO_3-oxidized activated carbon support (AC3) and/or with oxygen species adsorbed on Pt and Pt_3Sn alloy sites to weaken the oxidizing conditions offered by these species thus freeing some of the metallic sites for CO adsorption. The conversion of CO over 1wt%Pt-0.25wt%SnO_x supported on air-oxidized activated carbon (AC2) was also observed to increase with the addition of H_2, and the enhancement was only three fold (Acun, 2008). Increasing the H_2 content of the feed stream did not affect CO conversion. Catalyst characterization showed that PtSn alloy sites were more abundant on the AC2 support compared with Pt_3Sn alloy sites. Over 1wt%Pt-1wt%CeO_x/AC2 using the same air-oxidized AC2 support and CeO_x instead of SnO_x as promoter, on the other hand, the introduction of 10-60 mol% H_2 into the feed led to a gradual decrease in CO conversions and oxidation rates (Gülyüz *et al.* 2009). This finding was in agreement with reports suggesting that the mechanisms of CO oxidation over CeO_2-containing Pt catalysts may be quite different in the absence and presence of H_2.

4.5. The Effect of CO_2 on Low-Temperature CO Oxidation

Several experiments were performed in order to see the effect of CO_2 on the CO conversion over 1wt%Au-1.25wt%MgO/Al_2O_3 at 130°C by adding various concentrations of CO_2 (2, 4 and 6 mol%) to the feed. The CO conversions obtained from the experiments in the absence of H_2 are presented in Table 4.8 and plotted in Figure 4.8.

Table 4.8. CO conversions in the presence of CO_2 at 130°C and constant space time over 1wt%Au-1.25wt%MgO/Al_2O_3.

Exp. No	Total Flow ($ml.min^{-1}$)	Weight of Catalyst (mg)	Feed Composition (mol%) with He as Balance			X_{CO}
			CO	O_2	CO_2	
1	150	20	6	3	2	0.10
2	150	20	6	3	4	0.085
3	150	20	6	3	6	0.084
10*	150	20	6	3	0	0.13

*: Data from Table 4.3.

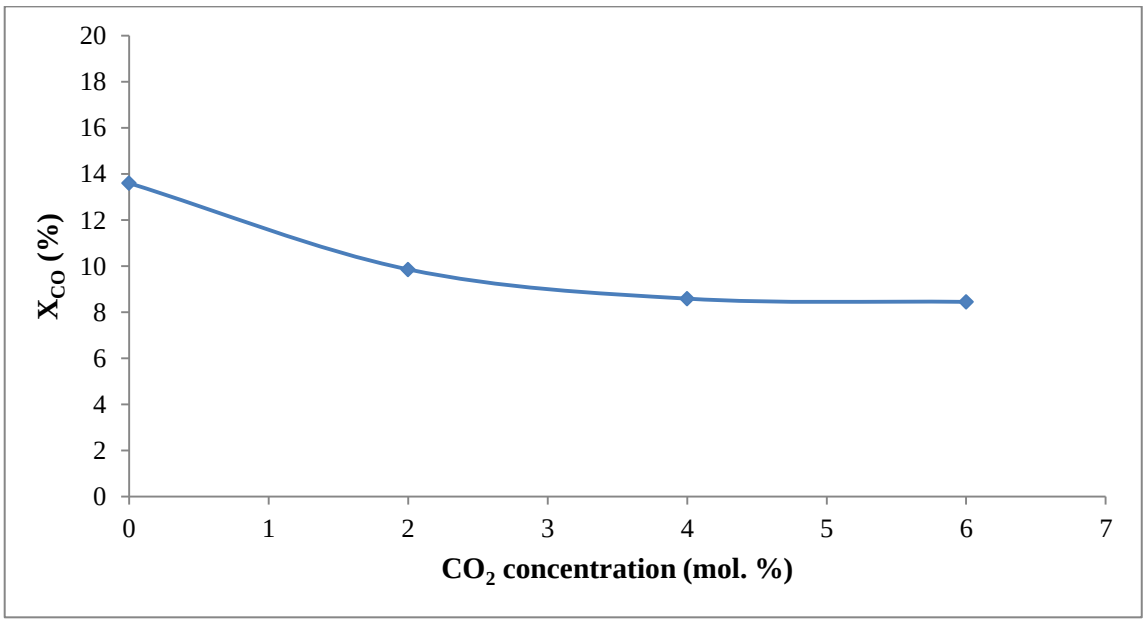

Figure 4.8. Effect of CO_2 on CO conversion over 1wt%Au-1.25wt%MgO/Al_2O_3 at 130°C and constant space time.

Addition of CO_2 to the feed first reduced the CO conversion, but further increase in feed CO_2 concentration did not change the conversion. The CO conversion was 13% when there was no CO_2 in the feed. The addition of a small amount of CO_2 (2 mol%) led to a decrease in conversion to 10%; but, at higher CO_2 concentrations of 4 mol% and 6 mol%, the CO conversion level remained constant at 8.50%.

The exit gas stream coming from the reformer and WGS reactor in the fuel processing section normally includes 15–25 vol% CO_2. It is therefore important to know the effect of CO_2 on the performance of the catalyst. The presence of CO_2 detrimentally influences the CO conversion capacity of noble metal reducible oxide catalysts on conventional supports such as Al_2O_3, Fe_2O_3 or CeO_2 while those supported on MgO are almost unaffected (Şimşek *et al.*, 2007).

The effects of CO_2 in the feed on CO oxidation were examined over promoted Au/Al_2O_3 catalysts using a constant H_2O concentration of 10 mol% and changing the CO_2 concentration from 0 to 25%. It was observed that the CO conversion decreased with increasing CO_2 concentration in the feed from 0 to 5%. Further increase in CO_2 content, on the other hand, did not have any significant impact. A CO_2 concentration of only 5 mol% is sufficient for negative effects, which were ascribed to the reverse water-gas-shift (WGS) reaction, formation of carbonates and/or adsorbed carboxylates (Davran-Candan and Tezcanlı, 2011).

4.6. The Effect of H_2O on Low-Temperature CO Oxidation

The effect of the presence of H_2O on low-temperature CO oxidation was studied at 130^oC over 1wt%Au-1.25wt%MgO/Al_2O_3 using a fixed total flow rate of 150 $ml.min^{-1}$ of feed with 4 mol% CO, 2 mol% O_2, 20 mol% H_2 and different H_2O concentrations by partially replacing balance He. The CO conversions obtained are presented in Table 4.9 and plotted in Figure 4.9.

Table 4.9. CO conversions in the presence of H_2O at 130°C and constant space time over 1wt%Au-1.25wt%MgO/Al_2O_3.

Exp. No	Total Flow ($ml.min^{-1}$)	Weight of Catalyst (mg)	Feed Composition (mol%) with He as Balance				X_{CO}
			CO	O_2	H_2	H_2O	
1	150	20	4	2	20	2	0.44
2	150	20	4	2	20	4	0.57
3	150	20	4	2	20	6	0.51
7*	150	20	4	2	20	0	0.38

*: Data from Table 4.7.

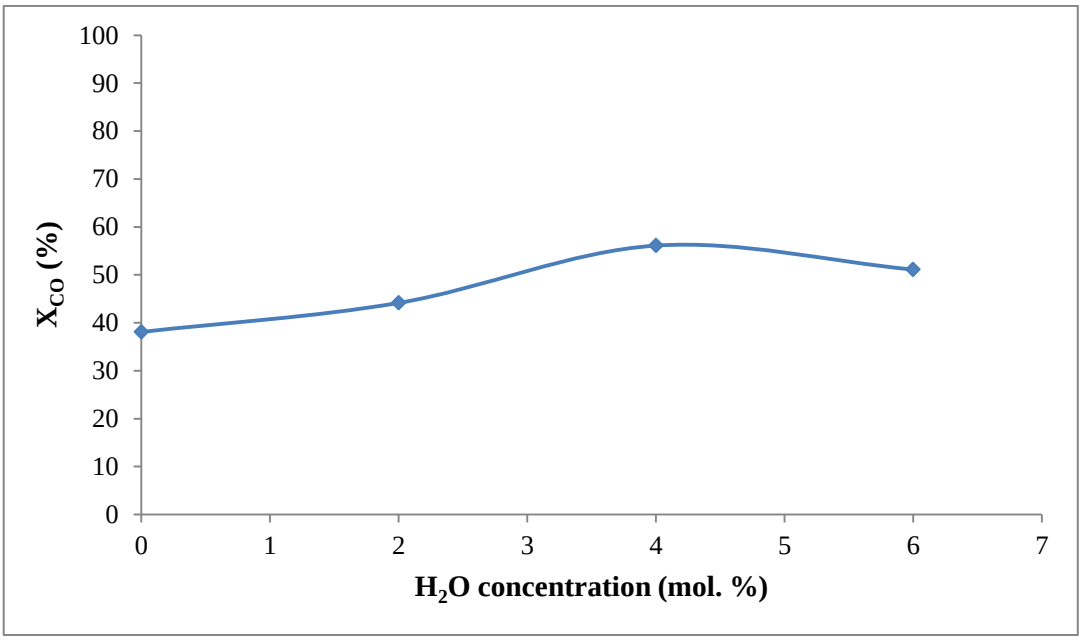

Figure 4.9. Effect of H_2O on CO conversion over 1wt%Au-1.25wt%MgO/Al_2O_3 at 130°C and constant space time.

Figure 4.9. shows that the introduction of H_2O into the feed up to 4 mol% enhances CO conversion in the presence of 4 mol% CO, 2 mol% O_2 and 20 mol% H_2, whereas further increases in H_2O concentarion start to have negative effects. CO conversion is 38% in the absence of H_2O. Addition of 2 mol% H_2O increases CO conversion to 44%, while a 4 mol% H_2O supplement further increases the conversion level to 57% (by almost 1.65). A

gradual decrease in CO conversion level starts with the addition of 6 mol% H_2O, although 51% conversion under these conditions is still higher than the 38% in the absence of H_2O.

The enhancement of CO conversion by the addition of H_2O to the feed was also observed on Au/MgO/γ-Al_2O_3 in the presence of 1% CO, 1% O_2, 60% H_2 and 25% CO_2 in the feed, concluding that the addition of H_2O not only balanced the inverse effect of CO_2, but also improved CO conversion further (Davran-Candan and Tezcanlı, 2011).

The activated carbon supported Pt-SnO_x and Pt-CeO_x catalysts were also positively influenced by the addition of H_2O into the feed for a few reasons. At suitable reaction temperatures, the presence of water vapor (i) promotes the WGS reaction leading more CO to be converted into CO_2, (ii) decreases the activation energy for CO oxidation, CO conversion is therefore increased greatly, and (iii) hydroxyl groups, which is formed by the dissociative adsorption of H_2O on Pt, also increase the oxidation rate of CO and H_2. Almost complete CO conversions were obtained at all times on stream implying that the presence of surface water also helps to remove CO via WGS activity (Şimşek *et al.*, 2007).

5. CONCLUSIONS AND RECOMMENDATIONS

5.1. Conclusions

In the present work, the kinetics of low temperature CO oxidation was studied over 1wt%Au-1.25wt%MgO/Al_2O_3 prepared by homogeneous deposition-precipitation. Firstly, preliminary experiments were conducted over 0.5wt%Au/Al_2O_3 at different total flow rates and catalyst amounts in order to determine the significance of physical transport effects in the microreactor flow system used and to ensure their absence in the 90-130^oC temperature range. The performance of 1wt%Au-1.25wt%MgO/Al_2O_3 at 130^oC was then examined for specific low temperature CO oxidation conditions by varying catalyst weight from 20 to 100 mg at stoichiometric and non-stoichiometric CO/O_2 ratios. Rates of CO oxidation were calculated in the initial rates region employing different initial CO and O_2 concentrations and CO/O_2 ratios. Experimental rate data were then used to estimate the kinetic parameters of power law type and LHHW type rate equations. Finally, the effects of H_2, CO_2 and H_2O in the feed on CO conversion in low-temperature CO oxidation were also studied. The following conclusions may be drawn:

- The performance of 1wt%Au-1.25wt%MgO/Al_2O_3 at 130^oC using different inlet CO concentrations and space times shows that CO conversion increases with increasing inlet CO concentration at a given value of W/F_{CO} for constant CO/O_2 ratios.
- Kinetics of low temperature CO oxidation over 1wt%Au-1.25wt%MgO/Al_2O_3 at 130^oC is well described by both power law and LHHW models.
- The reaction orders of the power law model are found as 0.61 and 0.36 for CO and O_2, respectively, indicating that the reaction takes place on a surface that is strongly adsorbed by oxygen with relatively weak CO adsorption.
- Statistical fit of two dual-site LHHW models to experimental data is rather good, indicating that two sites are involved per reaction cycle.
- Introduction of H_2 to the feed shows that H_2 has an enhancement effect on CO oxidation which gradually diminishes as H_2 concentration is increased.

- Addition of CO_2 has a negative effect on the conversion of low temperature CO oxidation. Small amounts of CO_2 in the feed (2-4 mol%) reduce CO conversion which, however, remains unchanged with further increase in CO_2 content.
- Addition of water vapor into CO, O_2 and H_2 containing feed also has an enhancement effect on CO conversion which gradually declines as H_2O content is increased but still remains above the CO conversion levels attained in its absence.

5.2. Recommendations

According to the results of the present study, the following points are thought to be beneficial for future work on kinetics of low-temperature CO oxidation:

- Additional experiments can be carried out by including H_2, CO_2 and H_2O in the feed in order to investigate the reaction rate dependency providing further insight into more conclusive reaction mechanisms and rate expressions.
- Kinetic experiments can be conducted at different temperatures to evaluate catalyst performance as well as to calculate the activation energy of low temperature CO oxidation, and to observe possible temperature effects on the reaction mechanism over 1wt%Au-1.25wt%MgO/Al_2O_3.

REFERENCES

Acun, S., 2008, "*Kinetics of Low Temperature CO Oxidation over Activated Carbon Supported Pt-SnO_x Catalysts"*, M. S. Thesis, Bogazici University, Istanbul.

Aguilar-Guerrero, V. and B. C. Gates, 2008, "Kinetics of CO Oxidation Catalyzed by Highly Dispersed CeO_2-Supported Gold", *Journal of Catalysis*, Vol. 260, pp. 351-357.

Avcı, A. K., L. David, Z. İ. Önsan, 2002, "Quantitative Investigation of Catalytic Natural Gas Conversion for Hydrogen Fuel Cell Applications", *Chemical Engineering Journal*, Vol. 90, pp. 77-87.

Azar, M., V. Caps, F. Morfin, J. Rousset, A. Piednoir, J. Bertolini and L. Piccolo, 2006, "Insights into Activation, Deactivation and Hydrogen-Induced Promotion of a Au/TiO_2 Reference Catalyst in CO Oxidation", *Journal of Catalysis*, Vol. 239, pp. 307-312.

Bartels, J. R., M. B. Pate and N. K. Olson, 2010, "An Economic Survey of Hydrogen Production from Conventional and Alternative Energy Sources", *International Journal of Hydrogen Energy*, Vol. 35, pp. 8371-8384.

Başar, M. S., 2010, "*Design, Construction and Testing of a Lab Scale Fuel Processor Prototype for Dynamic Performance Studies*", M. S. Thesis, Bogazici University, Istanbul.

Calla, J., M. Bore, A. Datye and R. Davis, 2006, "Effect of Alumina and Titania on the Oxidation of CO over Au Nanoparticles Evaluated by 13C Isotopic Transient Analysis", *Journal of Catalysis*, Vol. 238, pp. 458-467.

Centeno, M. A., M. Paulis, M. Montes and J. A. Odriozola, 2002, "Catalytic Combustion of Volatile Organic Compounds on $Au/CeO_2/Al_2O_3$ and Au/Al_2O_3 Catalysts", *Applied Catalysis A: General*, Vol. 234, pp. 65-78.

Chang, C.-T., B.-J. Liaw, C.-T. Huang and Y.-Z. Chen, 2007, "Preparation of Au/Mg_xAlO Hydrotalcite Catalysts for CO Oxidation", *Applied Catalysis A: General*, Vol. 332, pp. 216-224.

Chang, L.-H., Y.-L. Yeh and Y.-W. Chen, 2008, "Preferential Oxidation of CO in Hydrogen Stream over Nano-Gold Catalysts Prepared by Photodeposition Method", *International Journal of Hydrogen Energy*, Vol. 33, pp. 1965-1974.

Chang, L.-H., N. Sasirekha and Y.-W. Chen, 2007, "Au/MnO_2-TiO_2 Catalyst for Preferential Oxidation of Carbon Monoxide in Hydrogen Stream", *Catalysis Communications*, Vol. 8, pp. 1702-710.

Chen, Y., B. Liaw and C. Huang, 2006, "Selective Oxidation of CO in Excess Hydrogen over CuO/$Ce_xSn_{1-x}O_2$ Catalysts", *Applied Catalysis A: General*, Vol. 302, pp. 168-176.

Choudhury, S., J. Rangarajan and R. Rengaswamy, 2005, "Step Response Analysis of Phosphoric Acid Fuel Cell (PAFC) Cathode through a Transient Model", *Journal of Power Sources*, Vol. 140, pp. 274-279.

Cho, S., J. Park, S. Choi and S. Kim, 2006, "Effect of Magnesium on Preferential Oxidation of Carbon Monoxide on Platinum Catalyst in Hydrogen-rich Stream", *Journal of Power Sources*, Vol. 156, pp. 260-266.

Çağlayan, B. S., A. K. Avcı, Z. İ. Önsan and A. E. Aksoylu, 2005, "Production of Hydrogen over Bimetallic Pt-Ni/δ-Al_2O_3 I. Indirect Partial Oxidation of Propane", *Applied Catalysis*, Vol. 280, pp. 181-188.

Davran-Candan, T., 2011, *"Experimental and Computational Study of Selective CO Oxidation over Au/Al_2O_3 Catalyst"*, Ph. D. Thesis, Bogazici University, Istanbul.

Davran-Candan, T., S. T. Tezcanlı and R. Yıldırım, 2011, "Selective CO Oxidation over Promoted Au/γ-Al_2O_3 Catalysts in the Presence of CO_2 and H_2O in the Feed", *Catalysis Communications*, Vol. 12, pp. 1149-1152.

Date, M. and M. Haruta, 2001, "Moisture Effect on CO Oxidation over Au/TiO_2 Catalyst", *Journal of Catalysis*, Vol. 224, pp. 221-224.

Demir, M., 2009, "*Kinetic Study of Selective CO Oxidation on Au/Al_2O_3 Catalyst"*, M. S. Thesis, Bogazici University, Istanbul.

Ersöz, A., H. Olgun and S. Özdoğan, 2006, "Reforming Options for Hydrogen Production from Fossil Fuels for PEM Fuel Cells", *Journal of Power Sources*, Vol. 154, pp. 67-73.

Ervin, G. S., A. Tompos, M. Hegedu's, A. Szegedi and J. L. Margitfalvi., 2007, "The Influence of Cooling Atmosphere after Reduction on the Catalytic Properties of Au/Al_2O_3 and Au/MgO Catalysts in CO Oxidation", *Applied Catalysis*, Vol. 320, pp. 114-121.

Fogler, H. S., 2006, "*Elements of Chemical Reaction Engineering*", Prentice-Hall, Englewood Cliffs, New Jersey.

Grisel, R. J. H. and B. E. Nieuwenhuys, 2001, "A Comparative Study of the Oxidation of CO and CH_4 over Au/MO_x/Al_2O_3 Catalysts", *Catalysis Today*, Vol. 64, pp. 69-81.

Grisel, R. J. H., C. J. Weststrate, A. Goossens, M. W. J. Crajé, A. M. V. D. Kraan and B. E. Nieuwenhuys, 2002, "Oxidation of CO over Au/MO_x/Al_2O_3 Multi-Component Catalysts in a Hydrogen-Rich Environment", *Reactions*, Vol. 72, pp. 123-132.

Gülyüz, B., Ş. Ö. Aydınoğlu, A. E. Aksoylu and Z. İ. Önsan, 2009, "Kinetics of CO Oxidation over Pt-CeO_x Supported on Air-Oxidized Activated Carbon", *Turkish Journal of Chemistry*, Vol. 33, pp. 589-598.

Hao, Y., M. Mihaylov, E. Ivanova, K. Hadjiivanov, H. Knozinger and B. Gates, 2009, "CO Oxidation Catalyzed by Gold Supported on MgO: Spectroscopic Identification of Carbonate-Like Species Bonded to Gold during Catalyst Deactivation", *Journal of Catalysis*, Vol. 261, pp. 137-149.

Holladay, J., E. Jones, D. R. Palo, M. Phels, Y. H. Chin, R. Dagle, J. Hu, Y. Wang and E. Baker, 2004, "Miniature Fuel Processors for Portable Fuel Cell Power Supplies", *Materials Research Society Symposium Proceedings*, Vol. 756, pp. 429-434

Huang, Y., A. Wang, X. Wang and T. Zhang, 2007, "Preferential Oxidation of CO under Excess H_2H_2 Conditions over Iridium Catalysts", *International Journal of Hydrogen Energy*, Vol. 32, pp. 3880-3886.

Ince, T., G. Uysal, A. N. Akın and R. Yıldırım, 2005, "Selective Low-Temperature CO Oxidation Over Pt-Co-Ce/Al_2O_3 in Hydrogen-Rich Streams", *Applied Catalysis A*: General, Vol. 292, pp. 171-176.

Iwasa, N., S. Arai and M. Arai, 2008, "Selective Oxidation of CO with Modified Pd/ZnO Catalysts in the Presence of H_2: Effects of Additives and Preparation Variables", *Applied Catalysis B: Environmental*, Vol. 79, pp. 132-141.

Kaytakoğlu, S. and L. Akyalçın, 2007, "Optimization of Parametric Performance of a PEMFC", *International Journal of Hydrogen Energy*, Vol. 32, pp. 4418-4423.

Kim, Y. H. and E. D. Park, 2010, "The Effect of the Crystalline Phase of Alumina on the Selective CO Oxidation in a Hydrogen-rich Stream over Ru/Al_2O_3", *Applied Catalysis B: Environmental*, Vol. 96, pp. 41-50.

Kirubakaran, A., S. Jain and R. K. Nema, 2009, "A Review on Fuel Cell Technologies and Power Electronic Interface", *Renewable and Sustainable Energy Reviews*, Vol. 13, pp. 2430-2440.

Ko, E., E. Park, K. Seo, H. Lee, D. Lee and S. Kim, 2006, "A Comparative Study of Catalysts for the Preferential CO Oxidation in Excess Hydrogen", *Catalysis Today*, Vol. 116, pp. 377-383.

Laguna, O. H., M. Centeno, G. Arzamendi, L. M. Gandía, F. Romero-Sarria and J. Odriozola, 2010, "Iron-Modified Ceria and Au/ceria Catalysts for Total and Preferential Oxidation of CO (TOX and PROX)", *Catalysis Today*, Vol. 157, pp. 155-159.

Li, M., Z. Wu, Z. Ma, V. Schwartz, D. R. Mullins, S. Dai and S. H. Overbury, 2009, "CO Oxidation on Au/$FePO_4$ Catalyst: Reaction Pathways and Nature of Au Sites", *Journal of Catalysis*, Vol. 266, pp. 98-105.

Lian, H., M. Jia, W. Pan, Y. Li, W. Zhang and D. Jiang, 2005, "Gold-Base Catalysts Supported on Carbonate for Low-Temperature CO Oxidation", *Catalysis Communications*, Vol. 6, pp. 47-51.

Lucas-Consuegra, de A., A. Princivalle, A. Caravaca, F. Dorado, C. Guizard, J. L. Valverde and P. Vernoux, 2010, "Preferential CO Oxidation in Hydrogen-rich Stream over an Electro Chemically Promoted Pt Catalyst", *Applied Catalysis B: Environmental*, Vol. 94, pp. 281-287.

Luengnaruemitchai, A., S. Osuwan and E. Gulari, 2004, "Selective Catalytic Oxidation of CO in the Presence of H_2 over Gold Catalyst", *International Journal of Hydrogen Energy*, Vol. 29, pp. 429-435.

Masashi, K., A. Watanabe, H. Uchida, H. Yamashita and M. Watanabe, 2005, "Reaction Mechanism of Preferential Oxidation of Carbon Monoxide on Pt, Fe and Pt-Fe/Mordenite Catalysts", *Journal of Catalysis*, Vol. 236, pp. 262-269.

Maximo, M., G. T. Baronetti, M. A. Laborde and F. J. Marino, 2008, "Kinetics of Preferential CO Oxidation in H_2 Excess (COPROX) over CuO/CeO_2 Catalysts", *International Journal of Hydrogen Energy*, Vol. 33, pp. 3538-3542.

Muraki, H., S. Matunaga, H. Shinjoh, M. S. Wainwright and D. L. Trimm, 1991, "The Effect of Steam and Hydrogen in Promoting the Oxidation of Carbon Monoxide over a Platinum on Alumina Catalyst", *Journal of Chemical Technology* & *Biotechnology,* Vol. 52, pp. 415-424.

Naknam, P., A. Luengnaruemitchai and S. Wongkasemjit, 2009, "Preferential CO Oxidation over Au/ZnO and Au/ZnO–Fe_2O_3 Catalysts Prepared by Photodeposition", *International Journal of Hydrogen Energy*, Vol. 34, pp. 9838-9846.

Neef, H. J., 2009, "International Overview of Hydrogen and Fuel Cell Research", *Energy*, Vol. 34, pp. 327-333.

Önsan, Z. İ., 2007, "Catalytic Processes for Clean Hydrogen Production from Hydrocarbons", *Turkish Journal of Chemistry,* Vol. 31, pp. 531-550.

Perez-Hernandez, R., A. Gutierrez-Martinez and C. Gutierrez-Wing, 2007, "Effect of Cu Loading on CeO_2 for Hydrogen Production by Oxidative Steam Reforming of Methanol", *International Journal of Hydrogen Energy,* Vol. 32, pp. 2888-2894.

Panzera, G., V. Modafferi, S. Candamanoa, A. Donato, F. Frusteri and P.L. Antonucci., 2004, "CO Selective Oxidation on Ceria-Supported Au Catalysts for Fuel Cell Application", *Journal of Power Sources*, Vol. 135, pp. 177-183.

Park, J., 2004, "Activity and Characterization of the Co-promoted $CuO/CeO_2/Al_2O_3$ Catalyst for the Selective Oxidation of CO in Excess Hydrogen", *Applied Catalysis A: General*, Vol. 274, pp. 25-32.

Park, W. J., H. J. Jeong, W. Yoon, C. Kim, D. Lee, Y. Park and Y. Rhee, 2005, "Selective Oxidation of CO in Hydrogen-rich Stream over Cu/Ce Catalyst Promoted with Transition Metals", *International Journal of Hydrogen Energy,* Vol. 30, pp. 209-220.

Parinyaswan, A., S. Pongstabodee and A. Luengnaruemitchai, 2006, "Catalytic Performances of Pt–Pd/CeO_2 Catalysts for Selective CO Oxidation", *International Journal of Hydrogen Energy*, Vol. 31, pp. 1942-1949.

Qian, K., W. Zhang, H. Sun, J. Fang, B. He, Y. Ma, Z. Jiang, S. Wei, J. Yang and W. Huang, 2010, "Hydroxyls-Induced Oxygen Activation on 'Inert' Au Nanoparticles for Low-Temperature CO Oxidation", *Journal of Catalysis*, Vol. 277, pp. 95-103.

Quinet, E., L. Piccolo, H. Daly, F.C. Meunier, F. Morfin, A. Valcarcel, F. Diehl, P. Avenier, V. Caps and J. Rousset, 2008a, "H_2-Induced Promotion of CO Oxidation over Unsupported Gold", *Catalysis Today*, Vol. 138, pp. 43-49.

Quinet, E., F. Morfin, F. Diehl, P. Avenier, V. Caps and J. Rousset, 2008b, "Hydrogen Effect on the Preferential Oxidation of Carbon Monoxide over Alumina-Supported Gold Nanoparticles", *Applied Catalysis B: Environmental*, Vol. 80, pp. 195-201.

Rossignol, C., S. Arrii, F. Morfin, L. Piccolo, V. Caps and J. Rousset, 2005, "Selective Oxidation of CO over Model Gold-Based Catalysts in the Presence of H_2", *Journal of Catalysis*, Vol. 230, pp. 476-483.

Sebastian, V., S. Irusta, R. Mallada and J. Santamaría, 2009, "Selective Oxidation of CO in the Presence of H_2, CO_2 and H_2O, on Different Zeolite-supported Pt Catalysts", *Applied Catalysis A: General*, Vol. 366, pp. 242-251.

Seo, J. G., M. H. Youn, J. C. Jung and I. K. Song, 2009, "Effect of Preparation Method of Mesoporous Ni-Al_2O_3 Catalysts on Their Catalytic Activity for Hydrogen Production by Steam Reforming of Liquefied Natural Gas (LNG)", *International Journal of Hydrogen Energy*, Vol. 34, pp. 5409-5416.

Schoots, K., G. J. Kramer and B. C. C. van der Zwaan, "Technology Learning for Fuel Cells: Anassessment of Past and Potential Cost Reductions", *Energy Policy*, Vol. 38, pp. 2887-2897.

Schubert, M. M., A. Venugopal, M. J. Kahlich, V. Plzak and R. J. Behm, 2004, "Influence of H_2O and CO_2 on the Selective CO Oxidation in H_2-Rich Gases over Au/α-Fe_2O_3", *Journal of Catalysis*, Vol. 222, pp. 32-40.

Schubert, M. M., M. J. Kahlich, H. A. Gasteiger and R. J. Behm, 1999, "Correlation between CO Surface Coverage and Selectivity/Kinetics for the Preferential CO Oxidation over Pt/γ-Al_2O_3 and Au/α-Fe_2O_3: an in-situ DRIFTS Study", *Journal of Power Sources*, Vol.84, pp. 175-182.

Schumacher, B., Y. Denkwitz, V. Plzak, M. Kinne and R. J. Behm, 2004, "Kinetics, Mechanism and the Influence of H_2 on the CO Oxidation Reaction on a Au/TiO_2 Catalyst", *Journal of Catalysis*, Vol. 224, pp. 449-462.

Sollogoub, C., A. Guinault, C. Bonnebat, M. Bennjima, L. Akrour, J. F. Fauvarque and L. Ogier, 2009, "Formation and Characterization of Crosslinked Membranes for Alkaline Fuel Cells", *Journal of Membrane Science*, Vol. 335, pp. 37-42.

Souza, M., N. Ribeiro and M. Schmal, 2007, "Influence of the Support in Selective CO Oxidation on Pt Catalysts for Fuel Cell Applications", *International Journal of Hydrogen Energy*, Vol. 32, pp. 425-429.

Soyal-Baltacıoğlu, F. S., B. Gülyüz, A. E. Aksoylu and Z.İ. Önsan, 2007, "Low Temperature CO Oxidation Kinetics over Activated Carbon Supported Pt-SnO_x Catalysts", *Turkish Journal of Chemistry*, Vol. 31, pp. 455-464.

Şimşek, E., Ş. Özkara, A. E. Aksoylu and Z.İ. Önsan, 2007,"Preferential CO Oxidation over Activated Carbon Supported Catalysts in H_2-rich Gas Streams Containing CO_2 and H_2O", *Applied Catalysis A: General*, Vol. 316, pp. 169–174.

Tezcanlı, S. T., 2008, "*Au-based Catalyst Design for Selective CO Oxidation in Hydrogen-Rich Streams"*, M. S. Thesis, Bogazici University, Istanbul.

Thiam, H. S., W. R. W. Daud, S. K. Kamarudin, B. Mohammad, H. Kadhum, K. S. Loh and E. H. Majlan, 2011, "Overview on Nanostructured Membrane in Fuel Cell Applications", *International Journal of Hydrogen Energy*, Vol. 36, pp. 3187-3205.

Tomska-Foralewska, I., M. Zieliński, M. Pietrowski, W. Przystajko and M. Wojciechowska, 2011, "Iridium Supported on MgF_2–MgO as Catalyst for CO Oxidation", *Catalysis Today*, Vol. 4, pp. 10-13.

Trimm, D.L., 2005, "Minimisation of Carbon Monoxide in a Hydrogen Stream for Fuel Cell Application", *Applied Catalysis A: General*, Vol. 296, pp. 1-11.

Trimm, D. L. and Z. İ. Önsan, 2001, "Onboard Fuel Conversion for Hydrogen-Fuelcell-Driven Vehicles", *Catalysis Reviews*, Vol. 43, pp. 31-84.

Uysal, G., A. N. Akın, Z. İ. Önsan and R. Yıldırım, 2006, "Preferential CO Oxidation over Pt–SnO_2/Al_2O_3 in Hydrogen Rich Streams Containing CO_2 and H_2O (CO removal from H_2 with PROX)", *Catalysis Letters*, Vol. 111, pp. 173-176.

Varigonda, S. and M. Kamat, 2006, "Control of Stationary and Transportation Fuel Cell Systems: Progress and Opportunities", *Computers & Chemical Engineering*, Vol. 30, pp. 1735-1748.

Vázquez-Zavala, A., J. García-Gómez, A. Gómez-Cortés, 2000, "Study of the Structure and Selectivity of Pt-Au Catalysts", *Applied Surface Science*, Vol. 167, pp. 177-183.

Vizcaino, A., A. Carrero and J. Calles, 2007, "Hydrogen Production by Ethanol Steam Reforming over Cu-Ni Supported Catalysts", *International Journal of Hydrogen Energy*, Vol. 32, pp. 1450-1461.

Wang, Y., K. S. Chen, J. Mishler, S. C. Cho and X. C. Adroher, 2011, "A Review of Polymer Electrolyte Membrane Fuel Cells: Technology, Applications and Needs on Fundamental Research", *Applied Energy*, Vol. 88, pp. 981-1007.

Wang, Y., J. Zhu, J. Zhang, L. Song, J. Hu, S. Ong and W. Ng, 2006, "Selective Oxidation of CO in Hydrogen-Rich Mixtures and Kinetics Investigation on Platinum-Gold Supported on Zinc Oxide Catalyst", *Journal of Power Sources*, Vol. 155, pp. 440-446.

Wang, D., Z. Hao, D. Cheng, X. Shi and C. Hu, 2003, "Influence of Pretreatment Conditions on Low-Temperature CO Oxidation over $Au/MO_x/Al_2O_3$ Catalysts", *Journal of Molecular Catalysis*, Vol. 200, pp. 229-238.

Wen-Yueh, Y., W.-S. Lee, C.-P. Yang and B.-Z. Wan, 2007, "Low-Temperature Preferential Oxidation of CO in a Hydrogen Rich Stream (PROX) over Au/TiO_2: Thermodynamic Study and Effect of Gold-Colloid pH Adjustment Time on Catalytic Activity", *Journal of the Chinese Institute of Chemical Engineers*, Vol. 38, pp. 151-160.

Xie, Y. and X. Xue, 2009, "Transient Modeling of Anode-Supported Solid Oxide Fuel Cells", *International Journal of Hydrogen Energy*, Vol. 34, pp. 6882-6891.

Yi-Fen, Y., P. Sangeetha and Y.-W. Chen, 2009, "Au/TiO_2 Catalysts Prepared by Photo-Deposition Method for Selective CO Oxidation in H_2 Stream", *International Journal of Hydrogen Energy*, Vol. 34, pp. 8912–8920.

Youn, M. H., J. G. Seo, J. C. Jung, S. Park, D. R. Park, S. B. Lee and I. K. Song, 2009, "Hydrogen Production by Auto-thermal Reforming of Ethanol over Ni Catalyst Supported on ZrO_2 Prepared by a Sol–gel Method: Effect of H_2O/P123 Mass Ratio in the Preparation of ZrO_2", *Catalysis Today*, Vol. 146, pp. 57-62.

Yu, L., G. Ren, M. Qin and X. Jiang, 2009, "Transport Mechanisms and Performance Simulations of a PEM Fuel Cell with Interdigitated Flow Field", *Renewable Energy*, Vol. 34, pp. 530-543.

Zhang, H., G. Lin and J. Chen, 2011, “Performance Analysis and Multi-Objective Optimization of a New Molten Carbonate Fuel Cell System”, *International Journal of Hydrogen Energy*, Vol. 36, pp. 4015-4021.

Zhou, S., Z. Yuan and S. Wang, 2006, “Selective CO Oxidation with Real Methanol Reformate over Monolithic Pt Group Catalysts: PEMFC Applications”, *International Journal of Hydrogen Energy*, Vol. 31, pp. 924-933.

Zou, X., S. Qi, Z., Suo, L. and F. Li, 2007, “Activity and Deactivation of Au/Al_2O_3 Catalyst for Low-Temperature CO Oxidation”, *Catalysis Communications*, Vol. 8, pp. 784-788.